Science Advances
AAAS

advances.sciencemag.org/cgi/content/full/6/48/eabd5575/DC1

Supplementary Materials for

Single-cell peripheral immunoprofiling of Alzheimer's and Parkinson's diseases

Thanaphong Phongpreecha, Rosemary Fernandez, Dunja Mrdjen, Anthony E. Culos, Chandresh Gajera, Adam M. Wawro, Natalie Stanley, Brice Gaudillière, Kathleen L. Poston, Nima Aghaeepour, Thomas J. Montine*

*Corresponding author. Email: tmontine@stanford.edu

Published 25 November 2020, *Sci. Adv.* **6**, eabd5575 (2020)
DOI: 10.1126/sciadv.abd5575

This PDF file includes:

Supplementary Materials

Supplementary Methods

1. Clinical diagnosis

A consensus panel consisting of one board-certified movement disorders neurologist or behavioral neurologist, one board-certified neuropsychologist, and other study personnel adjudicated the diagnosis for each participant. PD diagnosis was based on UK PD Society Brain Bank clinical diagnostic criteria *(42)*, as previously reported *(43)*. AD included patients with dementia likely due to AD pathology based on the NIH Alzheimer's Disease Diagnostic Guidelines *(44)*. Healthy controls were determined to have no neurodegenerative disease or concerning cognitive decline by history, a normal neurological exam, and cognitive test scores within 1.5 standard deviations from normative values.

2. Data preprocessing

The FCS files acquired on the CyTOF (HELIOS, software version 6.5.358 by Fluidigm, S. San Francisco) were bead normalized using Fluidigm software. The normalized files were then debarcoded using Fluidigm software and the unassigned events were removed. The debarcoded FCS files were gated on Flow-jo Version 10.4.1 to remove beads and doublets and then gated to DNA-high events. The data were then arcsinh transformed and percentile normalized. The percentile normalized FCS files were then gated to characterize a broad range of cell types and signaling molecules (Fig. S9). The gating strategy employed in Fig. S9 was chosen as previously described by the Human Immune Monitoring Center (HIMC), Stanford University (*46, 57*). The DNA-high events of each sample were gated for basophils and non-basophils. Non-basophils were gated downstream for monocytes, lymphocytes, $CD3^+$, $CD4^+$, $CD8^+$, B cells, NK cells, and

DCs. Each of these cell types was further divided into subpopulations. $CD4^+$ (effector, naive, central memory and effector memory), $CD8^+$ (effector, naive, central memory, and effector memory), and B cells (switched memory, IgD^+ memory B, naive, and IgD^-CD27^-) were gated using quadrants (Fig. S9). The median expression values of the functional proteins in the gated populations were used for any further analyses.

Six samples that had less than 45% of total cells in DNA-high population for any kind of stimulation condition were excluded from the study. Missing values after gating (~0.1% of the signals in the discovery cohorts) were due to insufficient cell counts and were addressed by mean imputation. A batch correction method, ComBat *(58)*, was applied to reduce the staining batch effect. Batch effect was eliminated as measured by principal variance component analysis *(59)*.

To confirm the subpopulation identity achieved using the gating strategy in Fig. S9, we also employed alternate gating parameters and applied them to 12 randomly selected (sex-matched, 6 HC and 6 AD) samples. The results are shown in Fig. S10. The alternate gating strategy had three steps. First, gates were adjusted to eliminate adjacent borders and ensure no overlap, because subpopulations may change from donor to donor and with stimulation *(57, 60)*. This included non-basophils, monocytes, lymphocytes, $CD4^+$, $CD8^+$, Tregs, B cells, non-BT, IgA^+ B cells, NK cells, DCs, pDCs, and mDCs. Second, the $CD56^+$ $CD3^+$ gate of NKT cells was revised to match the $CD56^+$ $CD3^-$ population. Third, all quadrants were removed and specific gates applied to the following subpopulations: $CD4^+$ (effector, naive, central memory and effector memory), $CD8^+$ (effector, naive, central memory and effector memory), and B cells (switched memory, IgD^+ memory B, naive, IgD^-CD27^- B cells). Comparing the resulting 4,200 median expression values of the original and alternate gating strategies showed less than 10% difference (excluding outliers) between the two gating strategies across all samples and cell types (Fig. S11, A-B). The % difference was defined as $2 \cdot \frac{|a-b|}{|a+b|} \times 100\%$, where a and b represent the values from the original gating strategy and the new values from the alternate gating strategy. Importantly, when these new median expression values were used as inputs to the iEN model (trained on data from the original gating strategy and used to generate the results shown in the main Figures) without any retraining or other changes, the model predicted clear separation between HC and AD (Fig. S11C). Thus, the response observed is consistent across gating strategies.

3. Model reduction

A one-hundred iteration bootstrapping procedure with replacement, each with a subset of patients equal to the size of the full dataset, was employed to identify the number of most significant components of the iEN model. A piecewise regression analysis *(61)* was then performed on the median *P* value of the model from all iterations as a function of the number of features to identify the number of most significant components.

4. Correlation network construction

The layout of the correlation network was obtained by applying a dimension reduction algorithm, t-SNE, on the Spearman correlation matrix of all available immune features. The edge of the graph represents those with Spearman's *P* value < 0.05 after Bonferroni adjustment. For visualization of the group of highly correlated immune features, the communities were identified by using uniform manifold approximation and projection (UMAP) to reduce the dimension to

10% of the original immune features, followed by unsupervised clustering using *K*-means algorithm. The optimized number of clusters (24 clusters) was determined based on optimized C-index and Baker-Hubert gamma index.

5. Evaluating pPLCγ2 signal as a stand-alone biomarker

As shown in Figure 4, panels I through K, we tested whether any one of the 280 pPLCγ2 immune features from different cell types and stimulating conditions was sufficient as a stand-alone biomarker without any machine learning. A 1000-iteration leave-group-out cross-validation strategy was used on the discovery cohort. In each iteration and for each feature, the selected pPLCγ2 feature values (or the iEN predicted values from the discovery cohort) were split into 9:1 training/testing set. The threshold that resulted in the highest AUC (top left part of the ROC curve) was established using the training set. The values in the testing set were binarized to 0 and 1 using the threshold and F1-score. A harmonic mean of precision and recall ($2 \cdot \frac{precision \times recall}{precision + recall}$), was calculated by comparing to the ground truth. After 1000 iterations, the thresholds from all iterations were averaged to yield the final threshold used for evaluating that feature against the validation cohort.

Supplementary Figures

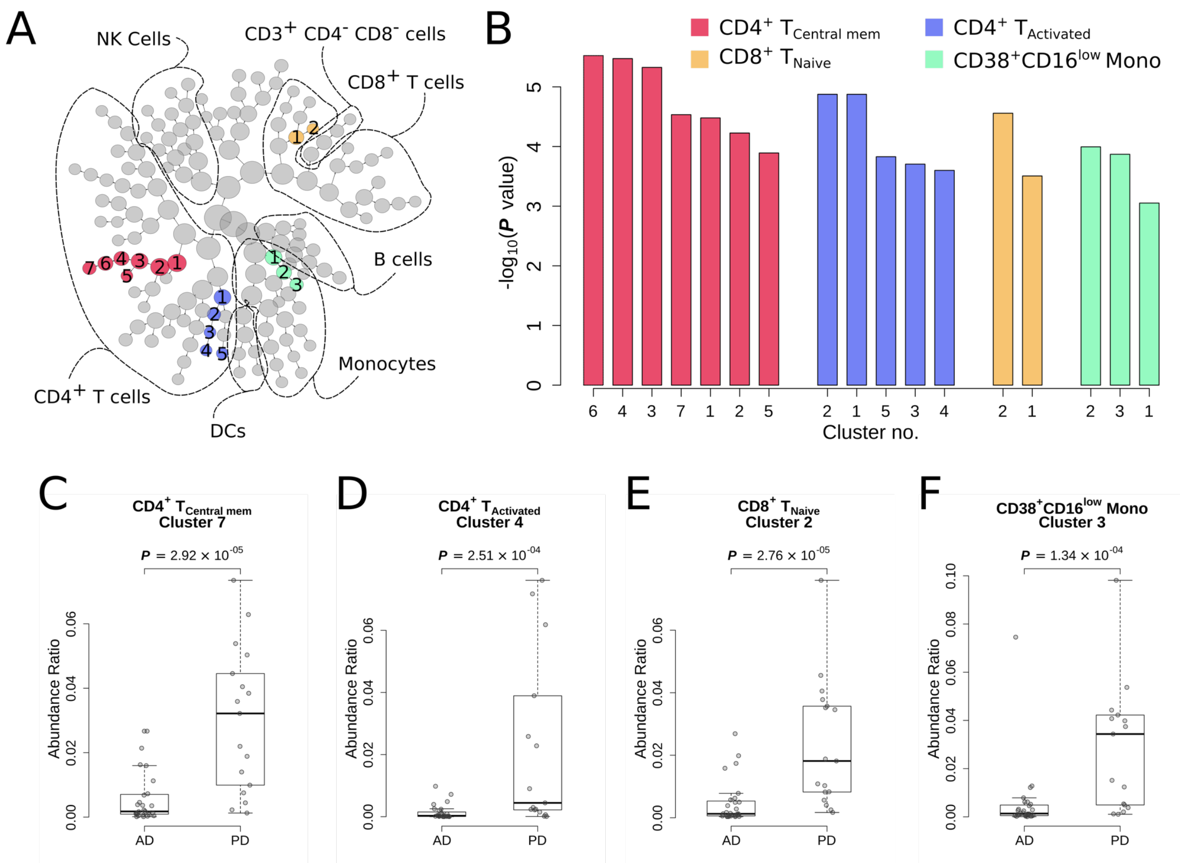

Fig. S1. Alzheimer's disease (AD) and Parkinson's disease (PD) patients exhibited different cell frequencies in several cell subsets. (**A**), CITRUS-derived dendrogram of unstimulated PBMC data from AD and PD. PBMC subsets are represented as clusters and color coded for level of marker expression (see Methods). Red-highlighted nodes are CD4$^+$ T$_{\mathrm{Central\ Mem}}$, blue-highlighted nodes are CD4$^+$ T$_{\mathrm{Activated}}$, orange-highlighted clusters are CD8$^+$ T$_{\mathrm{Naive}}$, and the green clusters are CD38$^+$CD16$^{\mathrm{low}}$ monocytes that were significantly different (q value < 0.05) between the two diagnostic groups. (**B**), Significance levels of the highlighted nodes. (**C–F**), Box plots presenting example values from the last node in each of the four highlighted lineages. *P* values for the stratified subsets were determined using Wilcoxon rank-sum test.

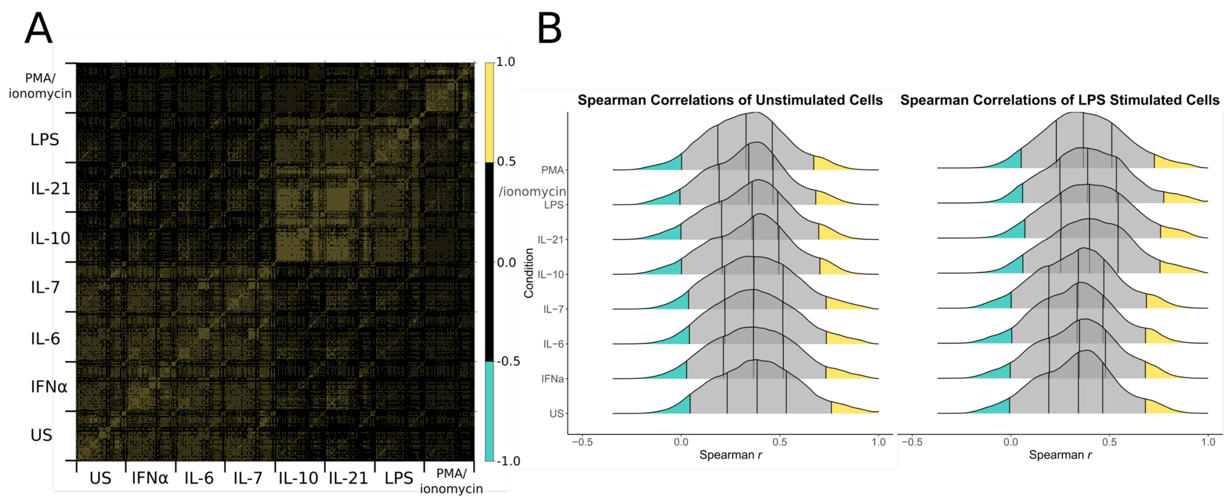

Fig. S2. Heatmap and distribution plots of Spearman *r* coefficients showing higher correlations among stimulation subsets. (**A**), Heatmap of the pair-wise correlations among the 4,200 immune features with some tending towards higher correlation coefficients (Spearman $r > 0.5$). The first are among cells from unstimulated (US), IFN-α, IL-6, and IL-7 stimulated conditions; the second are among IL-10, IL-21, LPS, and (to a lesser extent) PMA/ionomycin stimulated cells. (**B**), Examples of distribution plots showing higher quantiles of Spearman *r* between US condition with IFN-α, IL-6, and IL-7 (left), and a similar one for LPS with IL-10, IL-21, and PMA/ionomycin (right).

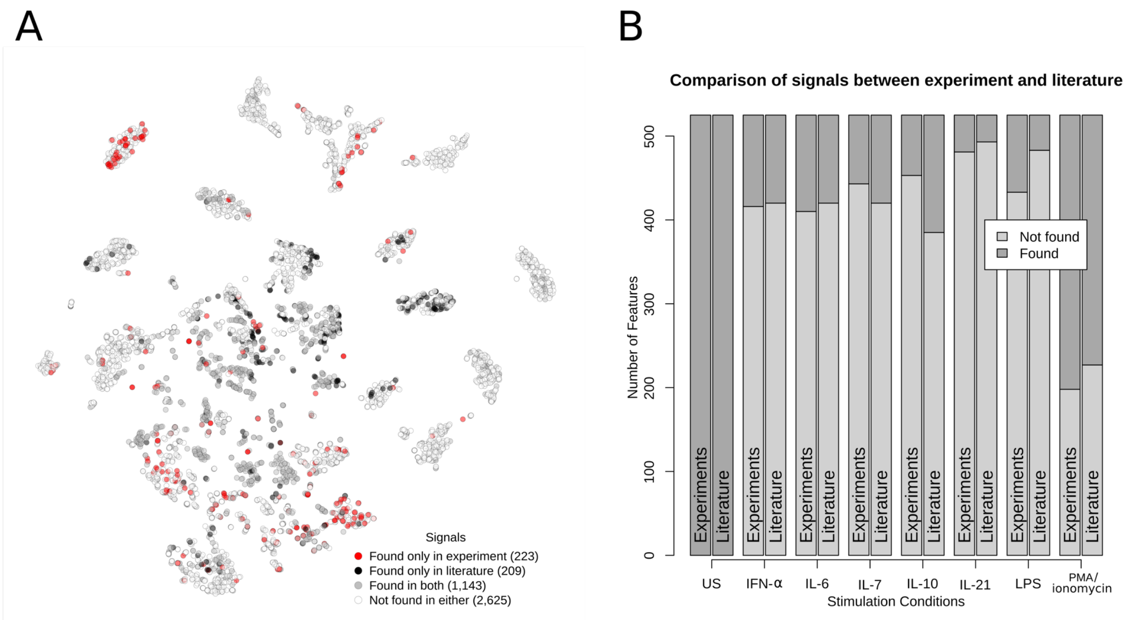

Fig. S3. Portions of canonical responses that were expected based on published literature vs. those observed experimentally in this study. (**A**), The correlation network colored by: responses that were expected based on published literature and also observed in this study (gray), those that were not expected from literature and were also not observed (white), and those that were expected from the literature but not observed experimentally or vice versa (black and red). (**B**), The portion of the responses that were expected based on published literature or observed experimentally in this study.

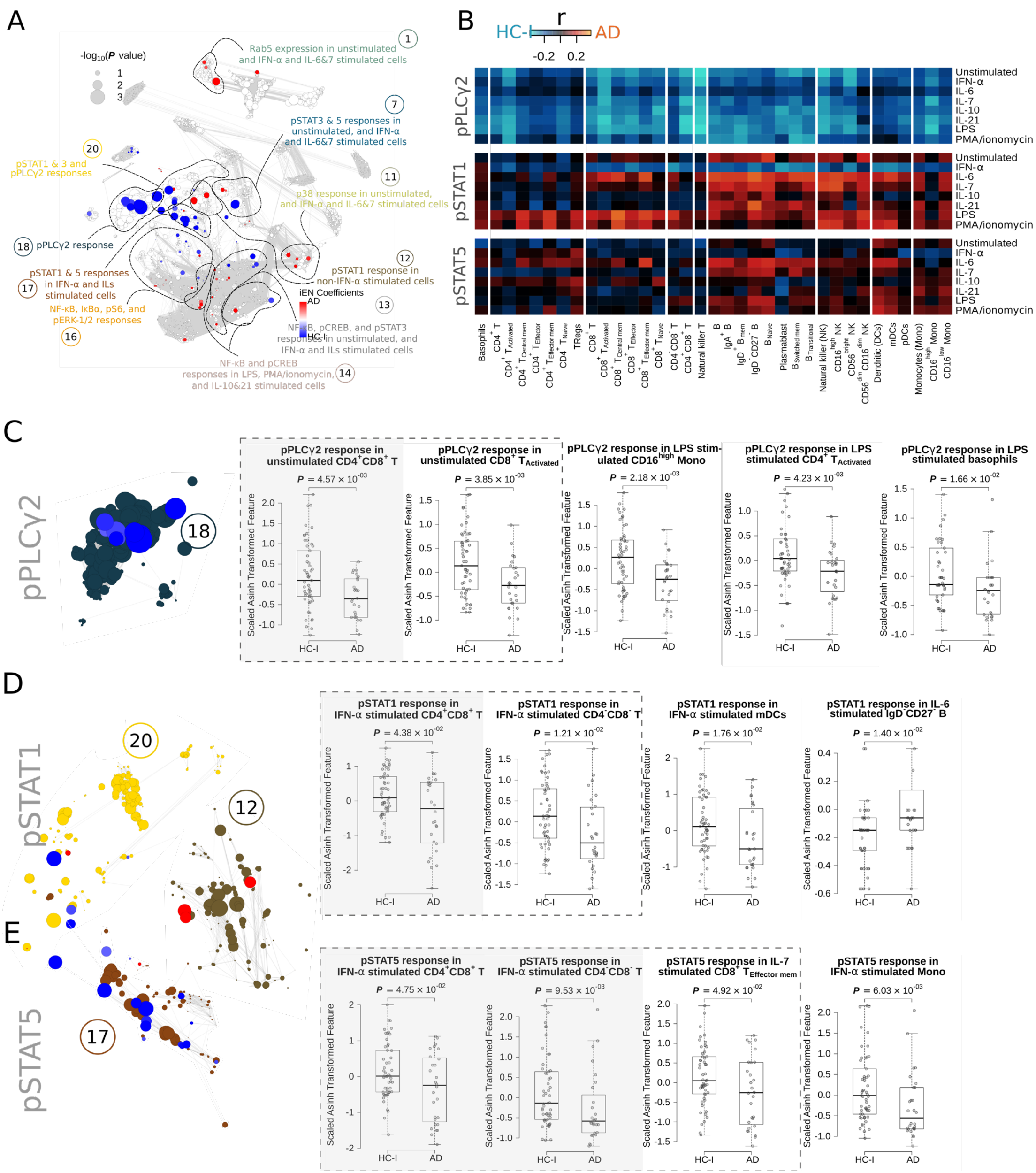

Fig. S4. Visualizations of features with strong signals and other features associated with the 111 top iEN selected components. (**A**), Network correlation with all the features associated with the top 111 iEN components colored. (**B**), heatmaps of the selected communities with magnitude colored by Spearman's correlation (r) coefficients. (**C–E**), Box plots of the selected features in the communities. The shaded gray areas indicate that the features are also a part of reduced iEN's top 14 components, and the boxes indicate features that are among the top 111 components.

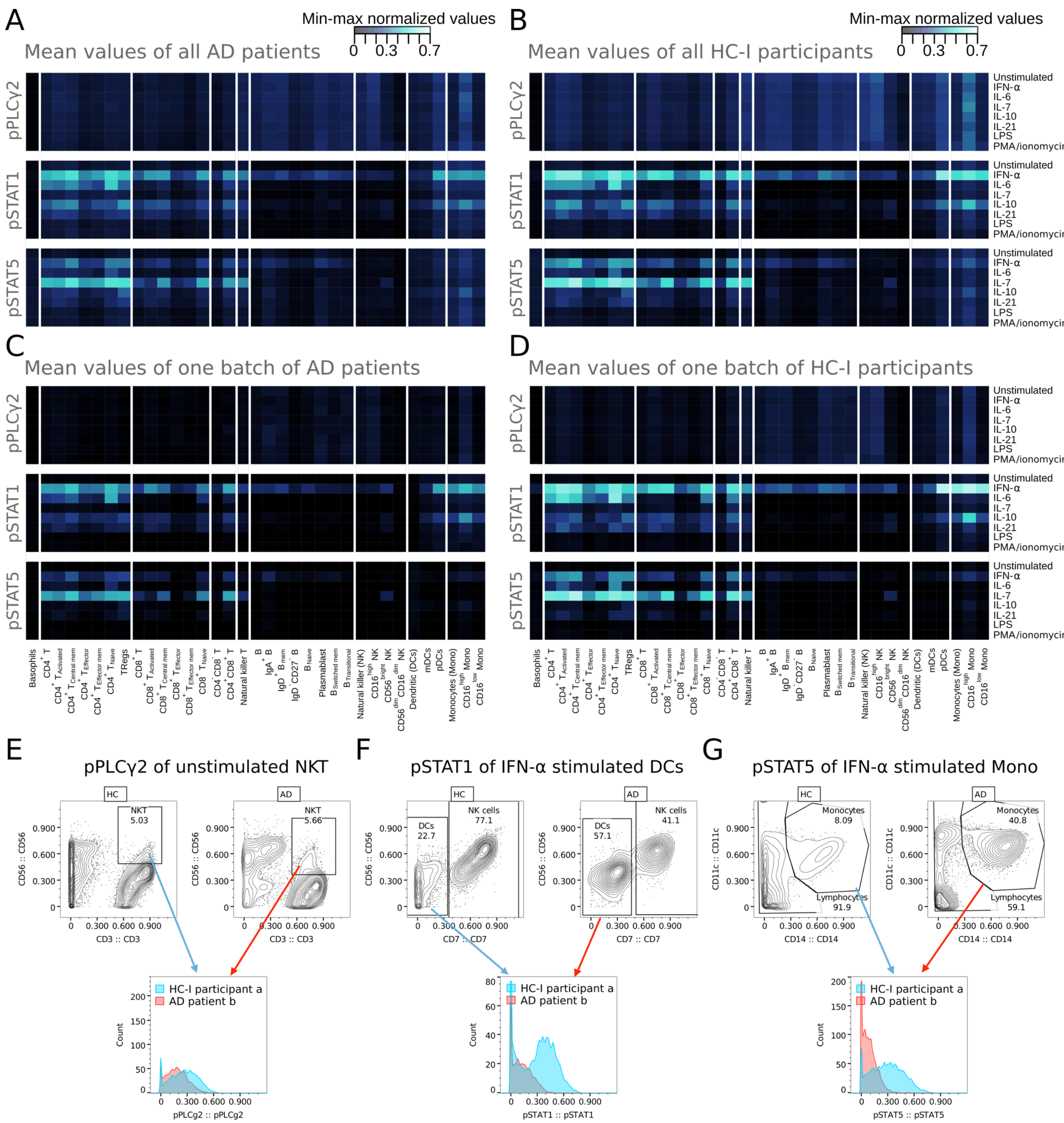

Fig. S5. Responses of pPLCγ2, pSTAT1, and pSTAT5 show expected expressions according to literature. (**A**), Heatmaps of the mean values of normalized responses in each cell subset and stimulation for all AD patients in the discovery cohorts before batch correction. (**B**), Similar to (**A**) but for HC-I participants. (**C**), Similar heatmap with only AD patients of the biggest batch in the discovery cohort. (**D**), Similar to (C), but for HC-I participants. (**E–G**), Examples of raw gated signals with a corresponding density plot from a pair of participants.

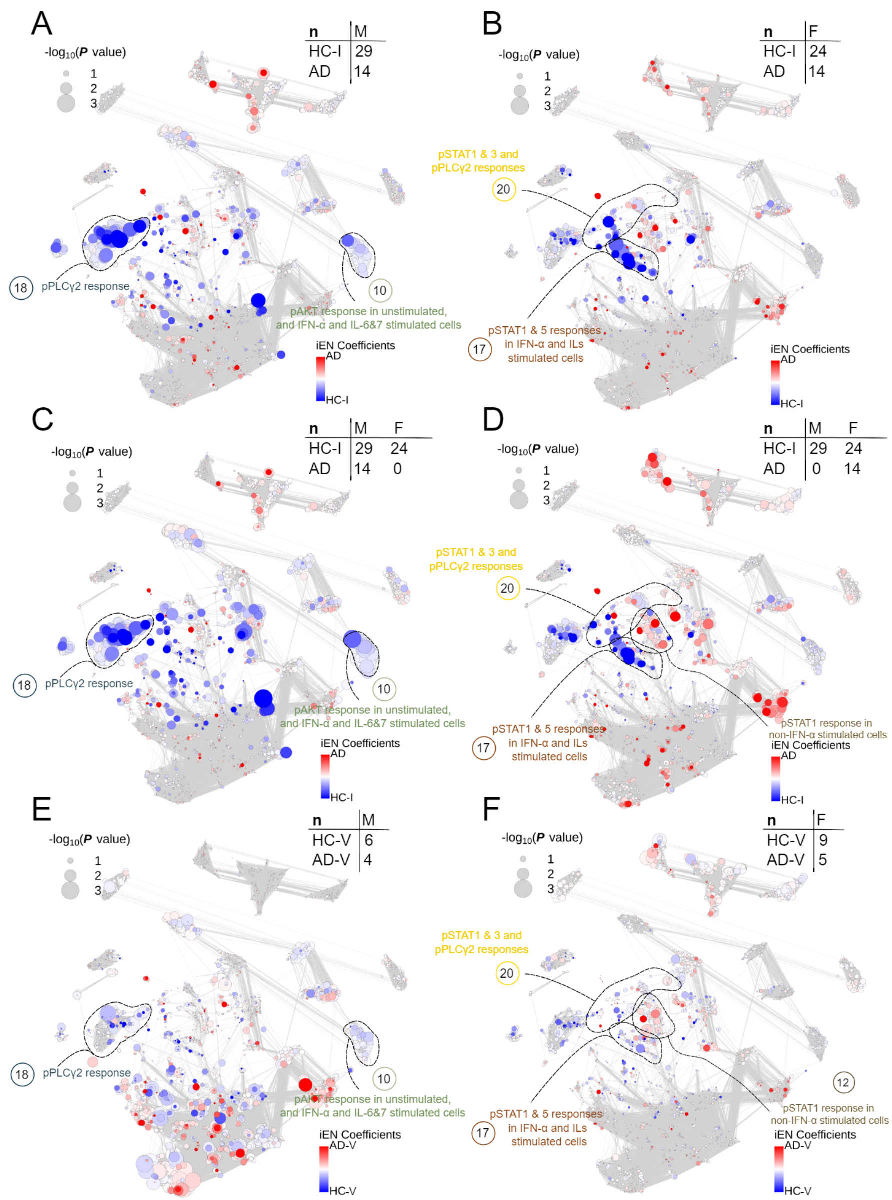

Fig. S6. Correlation network for AD/HC separated by sex. (**A-B**), The correlation network with node size corresponding to the Wilcoxon rank-sum test *P* value of each feature for AD/HC-I diagnosis in male and female participants (discovery cohort). (**C-D**), The similar correlation network for both sexes of healthy cohorts (HC-I) but for sex-specific AD. (**E-F**), The similar correlation network as (A-B) for the validation (V) data set. The color of each node represents the magnitude and direction of the associated iEN components developed from AD/HC-I classification model using all AD and HC-I data.

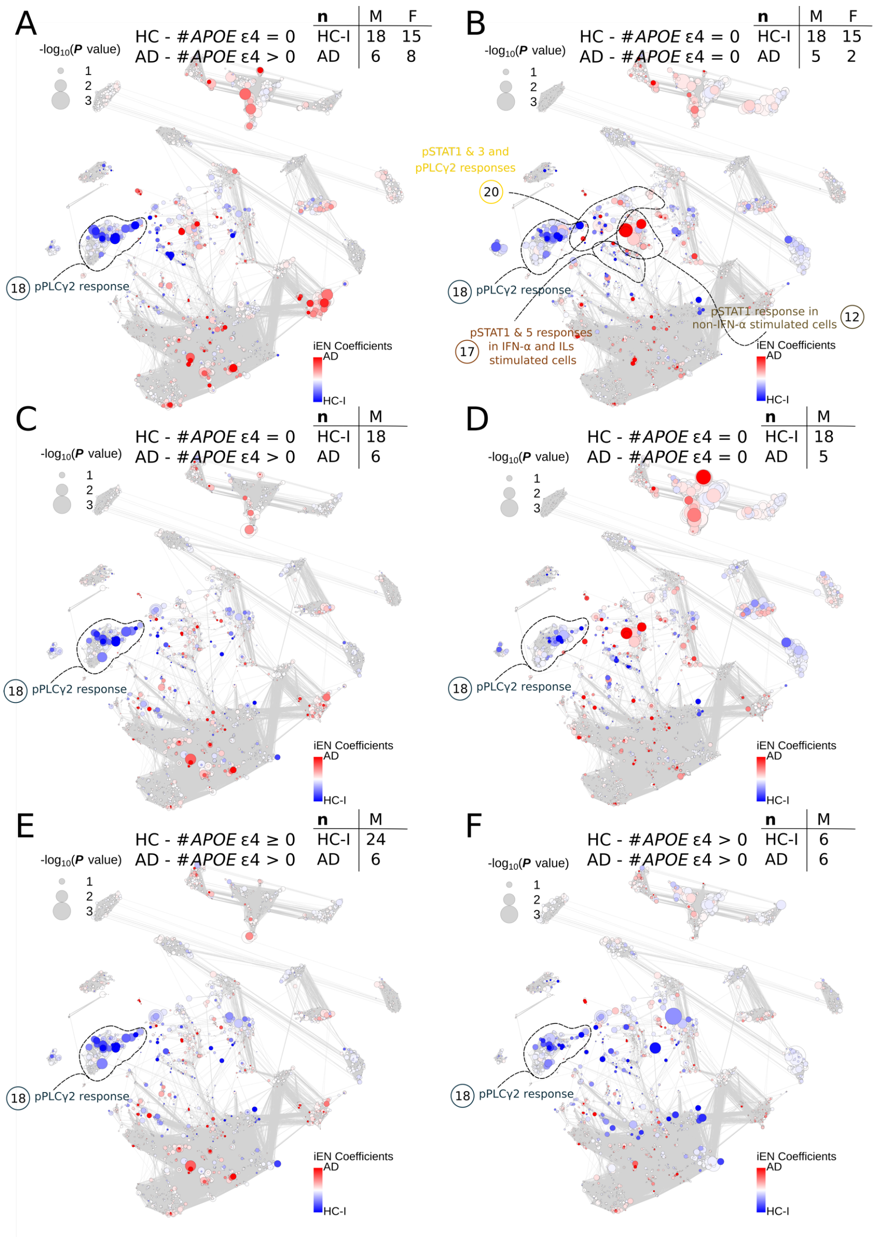

Fig. S7. Correlation network for *APOE* ε4- allele effects in AD/HC. (**A**), The correlation network of healthy cohorts (HC-I) with no *APOE* ε4 allele and Alzheimer's disease (AD) with at least one *APOE* ε4 allele. (**B**), Similar to (A), but for both groups with no *APOE* ε4 allele. (**C-D**), Similar correlation networks to (A) and (B) but for male participants only. (**E**), Similar correlation network to (C), but for all male HC-I. (**F**), A correlation network where all male participants have at least one *APOE* ε4 allele.

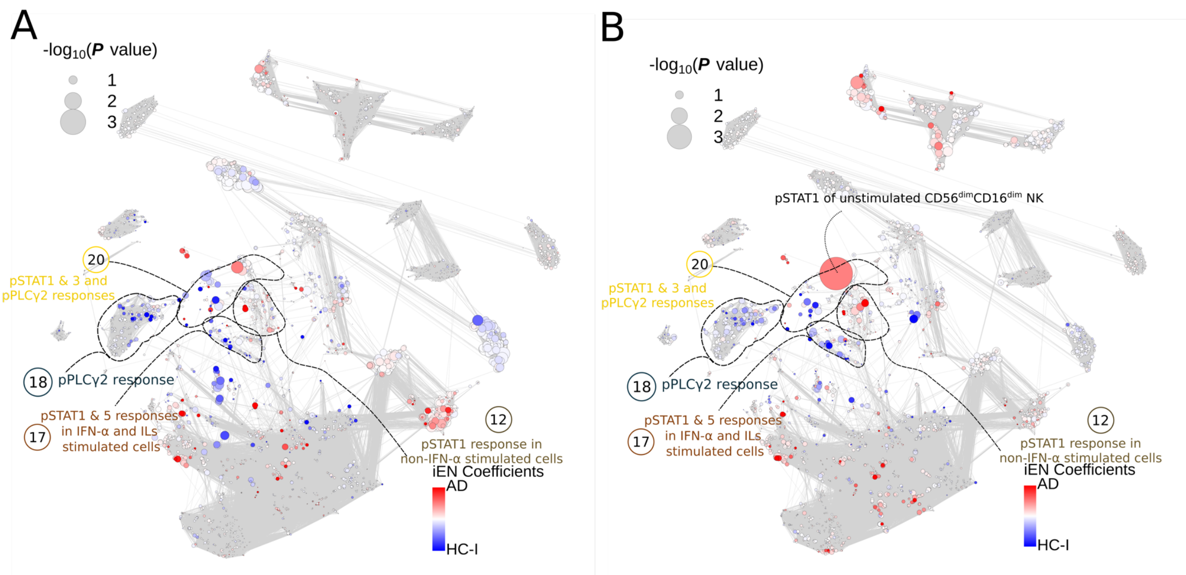

Fig. S8. Correlation network of HC-II/HC-I and HC-II/AD indicating that age does not share key differential pSTATs and pPLCγ2 signals highlighted by HC-I/AD. (**A**), The correlation network with node size corresponding to the Wilcoxon rank-sum test *P* value of each feature for HC-II/HC-I. The color of each node represents the magnitude and direction of the associated iEN components developed from AD/HC-I classification. (**B**), Similar to (A), but for the HC-II/AD pair.

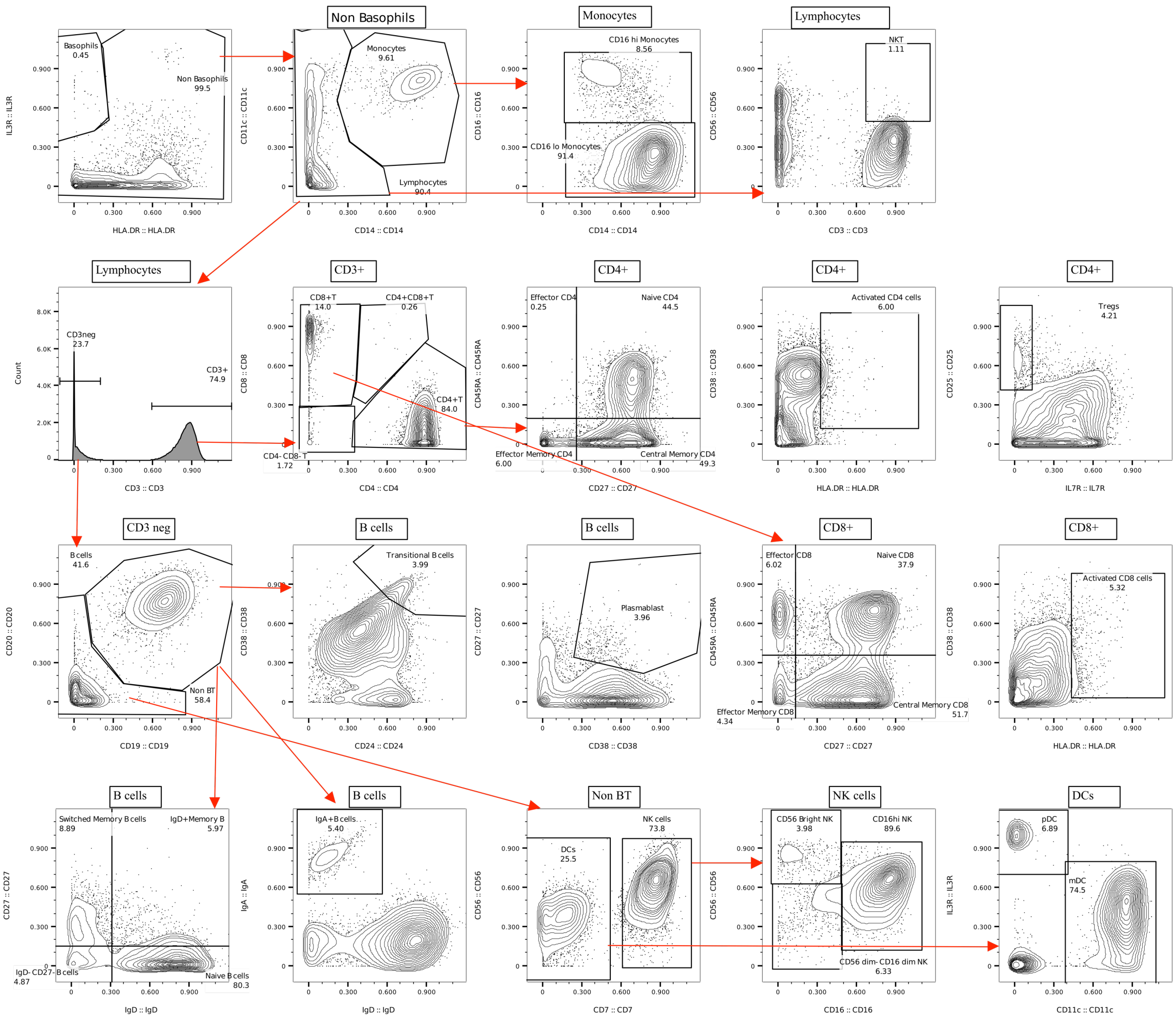

Fig. S9. Gating strategy to obtain different cell subsets. Thirty-five cell subsets were gated from PBMCs and a matrix of 12 phosphoepitopes and 3 endosomal proteins with 8 stimuli conditions evaluated from each subset. The DNA-high events of each sample were gated for basophils and non-basophils. Non-basophils were gated for monocytes, lymphocytes, CD3^{+}, CD4^{+}, CD8^{+}, B cells, NK cells, and DCs. Each of these cell types was further divided into subpopulations. CD4^{+} (effector, naive, central memory and effector memory), CD8^{+} (effector, naive, central memory and effector memory), and B cells (switched memory, IgD^{+} memory B, naive, IgD-CD27- B cells) were gated using quadrants.

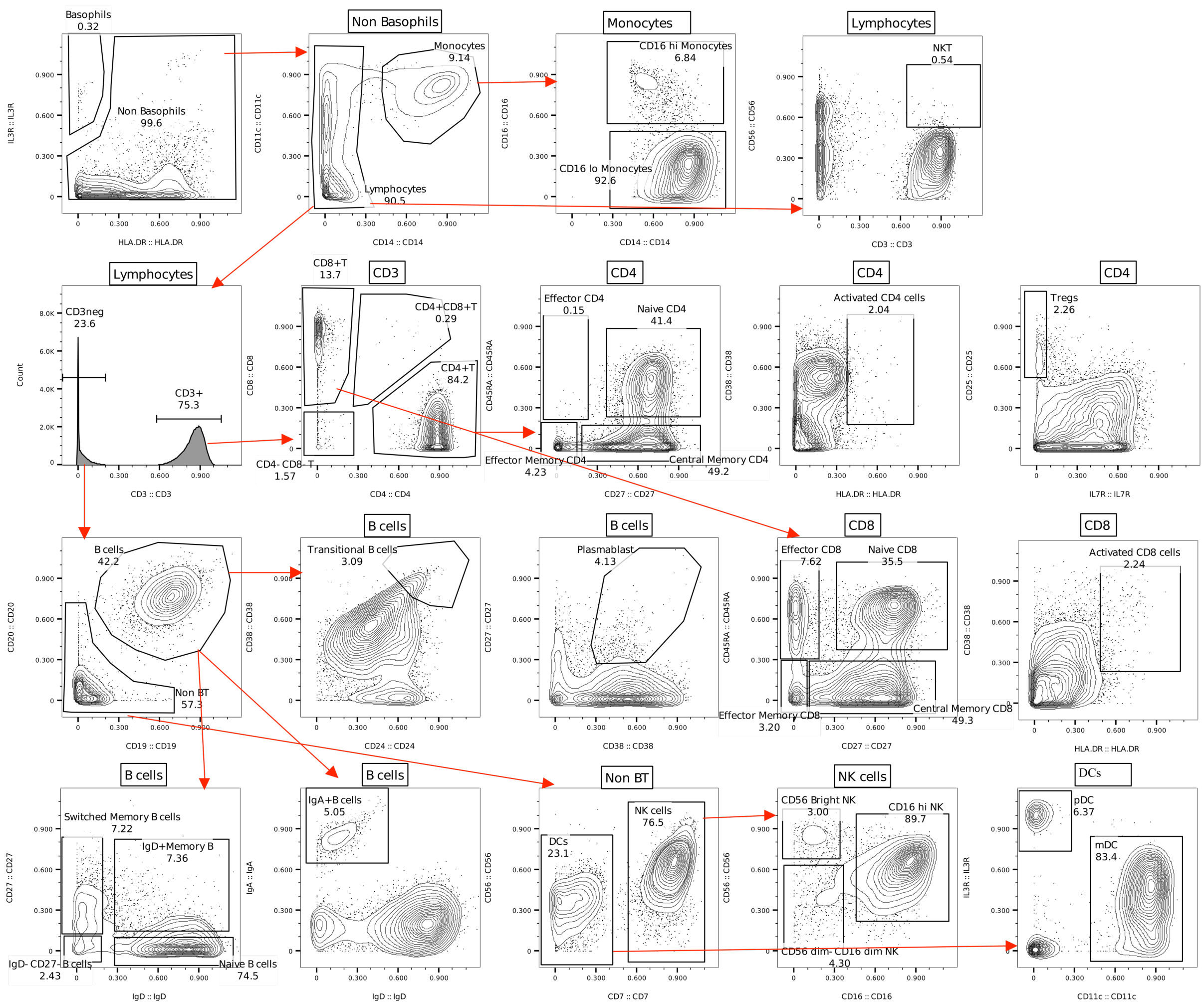

Fig. S10. Alternate gating process strategy to obtain different cell subsets. The same approach was used as in Fig. S9 with three modifications to the gating strategy: (i) Gates were adjusted to eliminate adjacent borders and ensure no overlap. This included non-basophils, monocytes, lymphocytes, CD4$^+$, CD8$^+$, Tregs, B cells, non-BT, IgA$^+$ B cells, NK cells, DCs, pDCs, and mDCs; (ii) The CD56$^+$ CD3$^+$ gate of NKT cells was revised to match the CD56$^+$ CD3$^-$ population; (iii) All quadrants were removed and specific gates applied to the following subpopulations: CD4+ (effector, naive, central memory and effector memory), CD8$^+$ (effector, naive, central memory and effector memory), and B cells (switched memory, IgD$^+$ memory B, naive, IgD$^-$CD27$^-$ B cells).

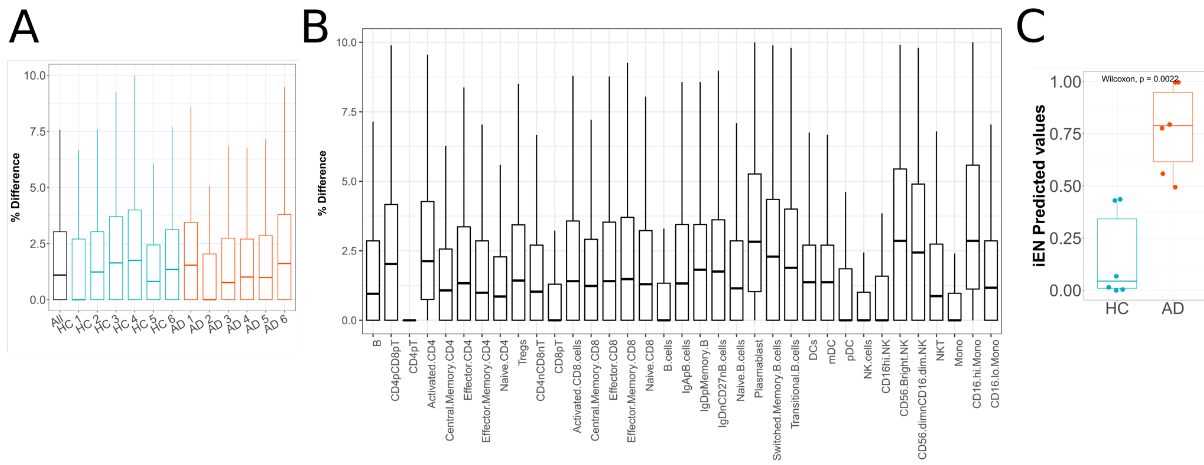

Fig. S11. Consistent response with original and alternate gating strategies. (**A**), Boxplot of percentage difference for each of the 4,200 median values resulting from the original (Fig. S9) and alternate (Fig. S10) gating schemes applied to each randomly selected sample. (**B**), Similar to (A), but stratified by cell type instead of sample. (**C**), iEN-predicted values from the alternate gating scheme using the iEN model developed from the original gating scheme.

Supplementary Tables

Table S1. Counts of each major cell type and their functional protein signals in each of the clusters in Fig. 2. US = unstimulated.								
Cluster 1 (n=143)								
Signal: Rab5 (n=140, 98%)								
	US	IFN-α	IL-6	IL-7	IL-10	IL-21	LPS	PMA/ Ionomycin
Basophils	1	1	1	1	-	-	-	-
CD4$^+$T	7	7	7	7	-	-	-	-
CD8$^+$T	6	6	6	6	-	-	-	-
CD4$^-$CD8$^-$T	1	1	1	1	-	-	-	-
CD4$^+$CD8$^+$T	1	1	1	1	-	-	-	-
NKT	1	1	1	1	-	-	-	-
B	8	8	8	8	-	-	-	-
NK	4	4	4	4	-	-	-	-
DCs	3	3	3	3	-	-	-	-
Monocytes	3	3	3	3	-	-	-	-
Signal: Lamp2 (n=3, 2%)								
	US	IFN-α	IL-6	IL-7	IL-10	IL-21	LPS	PMA/ Ionomycin
All	1	1	-	1	-	-	-	-
Cluster 2 (n=253)								
Signal: Lamp2 (n=253, 100%)								
	US	IFN-α	IL-6	IL-7	IL-10	IL-21	LPS	PMA/ Ionomycin
Basophils	1	1	1	1	1	1	1	1
CD4$^+$T	7	7	7	7	7	7	7	7
CD8$^+$T	6	6	6	6	6	6	6	6
CD4$^-$CD8$^-$T	1	1	1	1	1	1	1	1
CD4$^+$CD8$^+$T	1	1	1	1	1	1	1	1
NKT	1	1	1	1	1	1	1	1
B	7	7	8	7	8	8	8	8
NK	4	4	4	4	4	4	4	4
DCs	3	3	3	3	3	3	3	3
Monocytes	-	-	-	-	-	-	-	-

Cluster 3 (n=24)								
Signal: Lamp2 (n=24, 100%)								
	US	IFN-α	IL-6	IL-7	IL-10	IL-21	LPS	PMA/ Ionomycin
Basophils	-	-	-	-	-	-	-	-
$CD4^+T$	-	-	-	-	-	-	-	-
$CD8^+T$	-	-	-	-	-	-	-	-
$CD4^-CD8^-T$	-	-	-	-	-	-	-	-
$CD4^+CD8^+T$	-	-	-	-	-	-	-	-
NKT	-	-	-	-	-	-	-	-
B	-	-	-	-	-	-	-	-
NK	-	-	-	-	-	-	-	-
DCs	-	-	-	-	-	-	-	-
Monocytes	3	3	3	3	3	3	3	3

Cluster 4 (n=108)								
Signal: Rab5 (n=108, 100%)								
	US	IFN-α	IL-6	IL-7	IL-10	IL-21	LPS	PMA/ Ionomycin
Basophils	-	-	-	-	-	-	-	-
$CD4^+T$	-	-	-	-	5	5	5	5
$CD8^+T$	-	-	-	-	4	4	4	4
$CD4^-CD8^-T$	-	-	-	-	1	1	1	1
$CD4^+CD8^+T$	-	-	-	-	1	1	1	1
NKT	-	-	-	-	1	1	1	1
B	-	-	-	-	5	5	5	5
NK	-	-	-	-	4	4	4	4
DCs	-	-	-	-	3	3	3	3
Monocytes	-	-	-	-	3	3	3	3

Cluster 5 (n=32)								
Signal: Rab5 (n=32, 100%)								
	US	IFN-α	IL-6	IL-7	IL-10	IL-21	LPS	PMA/ Ionomycin
Basophils	-	-	-	-	1	1	1	1
$CD4^+T$	-	-	-	-	2	2	2	2
$CD8^+T$	-	-	-	-	2	2	2	2

$CD4^-CD8^-T$	-	-	-	-	-	-	-	-
$CD4^+CD8^+T$	-	-	-	-	-	-	-	-
NKT	-	-	-	-	-	-	-	-
B	-	-	-	-	3	3	3	3
NK	-	-	-	-	-	-	-	-
DCs	-	-	-	-	-	-	-	-
Monocytes	-	-	-	-	-	-	-	-

Cluster 6 (n=102)

Signal: ERK-1/2 (n=102, 100%)

	US	IFN-α	IL-6	IL-7	IL-10	IL-21	LPS	PMA/ Ionomycin
Basophils	-	-	-	-	1	1	1	1
$CD4^+T$	-	-	-	-	7	7	7	-
$CD8^+T$	-	-	-	-	6	6	6	-
$CD4^-CD8^-T$	-	-	-	-	1	1	1	-
$CD4^+CD8^+T$	-	-	-	-	1	1	1	-
NKT	-	-	-	-	1	1	1	-
B	-	-	-	-	8	8	8	-
NK	-	-	-	-	4	4	4	-
DCs	-	-	-	-	3	3	2	-
Monocytes	-	-	-	-	3	3	-	-

Cluster 7 (n=186)

Signal: pSTAT5 (n=102, 55%)

	US	IFN-α	IL-6	IL-7	IL-10	IL-21	LPS	PMA/ Ionomycin
Basophils	1	1	1	1	-	-	-	-
$CD4^+T$	7	-	5	-	-	-	-	-
$CD8^+T$	6	-	6	-	-	-	-	-
$CD4^-CD8^-T$	1	1	1	-	-	-	-	-
$CD4^+CD8^+T$	1	-	1	-	-	-	-	-
NKT	1	-	1	-	-	-	-	-
B	8	4	8	8	-	-	-	-
NK	4	4	4	3	-	-	-	-
DCs	3	3	3	3	-	-	-	-

Monocytes	3	3	3	3	-	-	-	-
Signal: pSTAT3 (n=72, 39%)								
	US	IFN-α	IL-6	IL-7	IL-10	IL-21	LPS	PMA/ Ionomycin
Basophils	1	1	1	1	-	-	-	-
$CD4^{+}T$	5	-	-	1	-	-	-	-
$CD8^{+}T$	6	-	4	5	-	-	-	-
$CD4^{-}CD8^{-}T$	1	-	1	1	-	-	-	-
$CD4^{+}CD8^{+}T$	1	-	-	1	-	-	-	-
NKT	1	-	-	1	-	-	-	-
B	5	-	6	6	-	-	-	-
NK	3	1	3	3	-	-	-	-
DCs	3	2	2	3	-	-	-	-
Monocytes	1	-	1	1	-	-	-	-
Signal: pSTAT1 (n=4, 2%)								
	US	IFN-α	IL-6	IL-7	IL-10	IL-21	LPS	PMA/ Ionomycin
All	1	-	-	1	-	-	1	1
Signal: NF-κβ (n=2, 1%)								
	US	IFN-α	IL-6	IL-7	IL-10	IL-21	LPS	PMA/ Ionomycin
All	-	1	-	1	-	-	-	-
Signal: p38 (n=2, 1%)								
	US	IFN-α	IL-6	IL-7	IL-10	IL-21	LPS	PMA/ Ionomycin
All	-	1	-	1	-	-	-	-
Signal: pLCK (n=2, 1%)								
	US	IFN-α	IL-6	IL-7	IL-10	IL-21	LPS	PMA/ Ionomycin
All	-	1	-	1	-	-	-	-
Signal: pCREB (n=1, 1%)								
	US	IFN-α	IL-6	IL-7	IL-10	IL-21	LPS	PMA/ Ionomycin
All	-	1	-	-	-	-	-	-
Signal: ERK-1/2 (n=1, 1%)								
	US	IFN-α	IL-6	IL-7	IL-10	IL-21	LPS	PMA/ Ionomycin

All	-	-	-	-	-	-	-	1

Cluster 8 (n=142)

Signal: EEA1 (n=140, 99%)

	US	IFN-α	IL-6	IL-7	IL-10	IL-21	LPS	PMA/ Ionomycin n
Basophils	1	1	1	1	-	-	-	-
$CD4^+T$	7	7	7	7	-	-	-	-
$CD8^+T$	6	6	6	6	-	-	-	-
$CD4^-CD8^-T$	1	1	1	1	-	-	-	-
$CD4^+CD8^+T$	1	1	1	1	-	-	-	-
NKT	1	1	1	1	-	-	-	-
B	8	8	8	8	-	-	-	-
NK	4	4	4	4	-	-	-	-
DCs	3	3	3	3	-	-	-	-
Monocytes	3	3	3	3	-	-	-	-

Signal: ERK-1/2 (n=2, 1%)

	US	IFN-α	IL-6	IL-7	IL-10	IL-21	LPS	PMA/ Ionomycin
All	-	1	-	1	-	-	-	-

Cluster 9 (n=138)

Signal: ERK-1/2 (n=138, 100%)

	US	IFN-α	IL-6	IL-7	IL-10	IL-21	LPS	PMA/ Ionomycin
Basophils	1	1	1	1	-	-	-	-
$CD4^+T$	7	7	7	7	-	-	-	-
$CD8^+T$	6	6	6	6	-	-	-	-
$CD4^-CD8^-T$	1	1	1	1	-	-	-	-
$CD4^+CD8^+T$	1	1	1	1	-	-	-	-
NKT	1	1	1	1	-	-	-	-
B	8	7	8	7	-	-	-	-
NK	4	4	4	4	-	-	-	-
DCs	3	3	3	3	-	-	-	-
Monocytes	3	3	3	3	-	-	-	-

Cluster 10 (n=138)

Signal: pAKT (n=138, 100%)

	US	IFN-α	IL-6	IL-7	IL-10	IL-21	LPS	PMA/ Ionomycin
Basophils	1	1	1	1	-	-	-	-
$CD4^+T$	7	7	7	7	-	-	-	-
$CD8^+T$	6	6	6	6	-	-	-	-
$CD4^-CD8^-T$	1	1	1	1	-	-	-	-
$CD4^+CD8^+T$	1	1	1	1	-	-	-	-
NKT	1	1	1	1	-	-	-	-
B	8	7	8	7	-	-	-	-
NK	4	4	4	4	-	-	-	-
DCs	3	3	3	3	-	-	-	-
Monocytes	3	3	3	3	-	-	-	-

Cluster 11 (n=154)

Signal: p38 (n=144, 94%)

	US	IFN-α	IL-6	IL-7	IL-10	IL-21	LPS	PMA/ Ionomycin
Basophils	1	1	1	1	-	-	-	-
$CD4^+T$	7	7	7	7	-	-	-	-
$CD8^+T$	6	6	6	6	-	-	-	-
$CD4^-CD8^-T$	1	1	1	1	-	-	-	-
$CD4^+CD8^+T$	1	1	1	1	-	-	-	-
NKT	1	1	1	1	-	-	-	-
B	8	7	8	7	-	-	-	-
NK	4	4	4	4	-	-	-	-
DCs	3	3	3	3	1	1	-	-
Monocytes	3	3	3	3	2	2	-	-

Signal: NF-κβ (n=5, 3%)

	US	IFN-α	IL-6	IL-7	IL-10	IL-21	LPS	PMA / Ionomycin
All	2	1	1	1	-	-	-	-

Signal: pSTAT3 (n=4, 3%)

	US	IFN-α	IL-6	IL-7	IL-10	IL-21	LPS	PMA / Ionomycin
All	2	-	-	2	-	-	-	-

Signal: pCREB (n=1, 1%)

	US	IFN-α	IL-6	IL-7	IL-10	IL-21	LPS	PMA / Ionomycin
All	-	-	-	1	-	-	-	-

Cluster 12 (n=128)

Signal: pSTAT1 (n=121, 95%)

	US	IFN-α	IL-6	IL-7	IL-10	IL-21	LPS	PMA / Ionomycin
Basophils	-	-	-	-	-	-	-	-
$CD4^+T$	4	-	-	6	-	-	7	5
$CD8^+T$	6	-	3	6	-	-	6	6
$CD4^-CD8^-T$	1	-	1	1	-	-	1	1
$CD4^+CD8^+T$	-	-	-	1	-	-	1	1
NKT	1	-	-	1	-	-	1	1
B	-	-	1	-	8	8	1	1
NK	-	-	-	-	3	2	-	-
DCs	3	-	3	3	-	3	3	3
Monocytes	3	-	3	3	-	3	3	3

Signal: pSTAT3 (n=5, 4%)

	US	IFN-α	IL-6	IL-7	IL-10	IL-21	LPS	PMA / Ionomycin
All	-	-	-	2	1	2	-	-

Signal: pSTAT5 (n=2, 2%)

	US	IFN-α	IL-6	IL-7	IL-10	IL-21	LPS	PMA / Ionomycin
All	-	-	-	-	1	1	-	-

Cluster 13 (n=335)

Signal: pCREB (n=137, 41%)

	US	IFN-α	IL-6	IL-7	IL-10	IL-21	LPS	PMA / Ionomycin
Basophils	1	1	1	1	-	-	-	-
$CD4^+T$	7	7	7	7	-	-	-	-
$CD8^+T$	6	6	6	6	-	-	-	-
$CD4^-CD8^-T$	1	1	1	1	-	-	-	1
$CD4^+CD8^+T$	1	1	1	1	-	-	-	-
NKT	1	1	1	1	-	-	-	-
B	8	7	8	7	-	-	-	-

NK	3	3	4	4	-	-	-	-
DCs	3	3	3	3	-	-	-	-
Monocytes	3	3	3	3	-	-	-	-
Signal: NF-κβ (n=96, 29%)								
	US	IFN-α	IL-6	IL-7	IL-10	IL-21	LPS	PMA / Ionomycin
Basophils	-	-	-	-	-	-	-	-
CD4^{+}T	5	5	5	5	-	-	-	-
CD8^{+}T	2	2	2	2	-	-	-	-
CD4^{-}CD8^{-}T	1	1	1	1	-	-	-	-
CD4^{+}CD8^{+}T	-	-	-	-	-	-	-	-
NKT	-	-	-	-	-	-	-	-
B	6	6	7	6	-	-	-	-
NK	4	4	4	4	-	-	-	-
DCs	2	3	3	3	1	1	1	1
Monocytes	2	2	2	2	-	-	-	-
Signal: pSTAT3 (n=70, 21%)								
	US	IFN-α	IL-6	IL-7	IL-10	IL-21	LPS	PMA / Ionomycin
Basophils	-	-	-	-	-	-	-	-
CD4^{+}T	-	6	3	-	7	6	-	-
CD8^{+}T	-	5	-	-	6	6	-	-
CD4^{-}CD8^{-}T	-	-	-	-	1	1	-	-
CD4^{+}CD8^{+}T	-	-	-	-	1	1	-	-
NKT	-	-	-	-	1	1	-	-
B	-	6	-	-	6	3	-	-
NK	-	-	-	-	3	3	-	-
DCs	-	-	-	-	1	-	-	-
Monocytes	-	-	-	-	3	-	-	-
Signal: IκBα (n=32, 10%)								
	US	IFN-α	IL-6	IL-7	IL-10	IL-21	LPS	PMA / Ionomycin
Basophils	-	-	-	-	-	-	-	-
CD4^{+}T	3	3	3	3	3	3	-	-
CD8^{+}T	-	-	-	-	-	-	-	-

CD4⁻CD8⁻T	-	-	-	-	-	-	-	-
CD4⁺CD8⁺T	-	-	-	-	-	-	-	-
NKT	-	-	-	-	-	-	-	-
B	-	-	-	-	-	-	-	-
NK	2	2	2	2	2	2	2	-
DCs	-	-	-	-	-	-	-	-
Monocytes	-	-	-	-	-	-	-	-

Cluster 14 (n=287)

Signal: pCREB (n=134, 47%)

	US	IFN-α	IL-6	IL-7	IL-10	IL-21	LPS	PMA / Ionomycin
Basophils	-	-	-	-	1	1	1	1
$CD4^+T$	-	-	-	-	7	7	7	7
$CD8^+T$	-	-	-	-	6	6	6	6
$CD4^-CD8^-T$	-	-	-	-	1	1	1	-
$CD4^+CD8^+T$	-	-	-	-	1	1	1	1
NKT	-	-	-	-	1	1	1	1
B	-	-	-	-	8	8	8	7
NK	-	-	-	-	4	4	4	3
DCs	-	-	-	-	3	3	3	1
Monocytes	-	-	-	-	3	3	3	2

Signal: NF-κβ (n=124, 43%)

	US	IFN-α	IL-6	IL-7	IL-10	IL-21	LPS	PMA / Ionomycin
Basophils	-	-	-	-	1	1	1	1
$CD4^+T$	1	1	1	1	7	7	7	7
$CD8^+T$	-	-	-	-	2	2	2	3
$CD4^-CD8^-T$	-	-	-	-	1	1	1	1
$CD4^+CD8^+T$	-	-	-	-	-	-	-	-
NKT	-	-	-	-	-	-	-	-
B	1	1	1	1	8	8	8	8
NK	-	-	-	-	4	4	4	4
DCs	-	-	-	-	2	2	2	2
Monocytes	1	1	-	1	3	3	3	3

Signal: p38 (n=24, 8%)

	US	IFN-α	IL-6	IL-7	IL-10	IL-21	LPS	PMA / Ionomycin
All	-	-	-	-	-	-	-	24

Signal: IκBα (n=4, 1%)

	US	IFN-α	IL-6	IL-7	IL-10	IL-21	LPS	PMA / Ionomycin
All	1	1	1	1	-	-	-	-

Signal: pSTAT3 (n=1, 0%)

	US	IFN-α	IL-6	IL-7	IL-10	IL-21	LPS	PMA / Ionomycin
All	-	-	-	-	-	1	-	-

Cluster 15 (n=250)

Signal: pLCK (n=249, 100%)

	US	IFN-α	IL-6	IL-7	IL-10	IL-21	LPS	PMA / Ionomycin
Basophils	-	-	-	-	-	-	-	-
$CD4^+T$	7	7	7	7	7	7	7	7
$CD8^+T$	6	5	5	6	6	6	6	6
$CD4^-CD8^-T$	1	1	1	1	1	1	1	1
$CD4^+CD8^+T$	1	1	1	1	1	1	1	1
NKT	-	-	-	1	1	-	-	-
B	7	7	8	7	7	7	7	7
NK	4	4	4	4	4	4	4	4
DCs	3	3	3	3	3	3	3	3
Monocytes	2	2	2	2	2	2	2	2

Signal: NF-κβ (n=1, 0%)

	US	IFN-α	IL-6	IL-7	IL-10	IL-21	LPS	PMA / Ionomycin
All	1	-	-	-	-	-	-	-

Cluster 16 (n=436)

Signal: IκBα (n=239, 55%)

	US	IFN-α	IL-6	IL-7	IL-10	IL-21	LPS	PMA / Ionomycin
Basophils	1	1	1	1	1	1	1	1
$CD4^+T$	3	3	3	3	4	4	7	7
$CD8^+T$	6	6	6	6	6	6	6	6

CD4⁻CD8⁻T	1	1	1	1	1	1	1	1
CD4⁺CD8⁺T	1	1	1	1	1	1	1	1
NKT	1	1	1	1	1	1	1	1
B	8	8	8	8	8	8	8	7
NK	2	1	1	2	2	2	2	4
DCs	3	3	3	3	3	3	3	3
Monocytes	3	3	3	2	3	3	2	3
Signal: NF-κβ (n=52, 12%)								
	US	IFN-α	IL-6	IL-7	IL-10	IL-21	LPS	PMA / Ionomycin
Basophils	-	-	-	-	-	-	-	-
CD4⁺T	1	1	1	1	-	-	-	-
CD8⁺T	4	4	4	4	4	4	4	3
CD4⁻CD8⁻T	-	-	-	-	-	-	-	-
CD4⁺CD8⁺T	1	1	1	1	1	1	1	1
NKT	1	1	1	1	1	1	1	1
B	-	-	-	-	-	-	-	-
NK	-	-	-	-	-	-	-	-
DCs	-	-	-	-	-	-	-	-
Monocytes	-	-	1	-	-	-	-	-
Signal: pS6 (n=47, 11%)								
	US	IFN-α	IL-6	IL-7	IL-10	IL-21	LPS	PMA / Ionomycin
Basophils	1	1	1	1	1	1	1	1
CD4⁺T	-	-	-	-	-	-	-	7
CD8⁺T	-	-	-	-	-	-	-	6
CD4⁻CD8⁻T	-	-	-	-	-	-	-	1
CD4⁺CD8⁺T	-	-	-	-	-	-	-	1
NKT	-	-	-	-	-	-	-	1
B	-	-	-	-	-	-	-	8
NK	-	-	-	-	-	-	-	4
DCs	1	1	1	1	1	1	1	1
Monocytes	-	-	-	-	-	-	-	3
Signal: ERK-1/2 (n=34, 8%)								

	US	IFN-α	IL-6	IL-7	IL-10	IL-21	LPS	PMA / Ionomycin
All	-	-	-	-	-	-	1	33
Signal: pLCK (n=29, 7%)								
	US	IFN-α	IL-6	IL-7	IL-10	IL-21	LPS	PMA / Ionomycin
All	4	4	4	2	3	4	4	4
Signal: pSTAT3 (n=17, 4%)								
	US	IFN-α	IL-6	IL-7	IL-10	IL-21	LPS	PMA / Ionomycin
All	-	9	7	-	1	-	-	-
Signal: p38 (n=14, 3%)								
	US	IFN-α	IL-6	IL-7	IL-10	IL-21	LPS	PMA / Ionomycin
All	-	-	-	-	-	-	4	10
Signal: pCREB (n=4, 1%)								
	US	IFN-α	IL-6	IL-7	IL-10	IL-21	LPS	PMA / Ionomycin
All	-	-	-	-	-	-	-	4
Cluster 17 (n=114)								
Signal: pSTAT1 (n=76, 67%)								
	US	IFN-α	IL-6	IL-7	IL-10	IL-21	LPS	PMA / Ionomycin
Basophils	-	-	-	-	-	-	-	-
$CD4^+T$	-	7	6	1	7	7	-	-
$CD8^+T$	-	6	-	-	6	6	-	-
$CD4^-CD8^-T$	-	1	-	-	1	1	-	-
$CD4^+CD8^+T$	-	1	-	-	1	1	-	-
NKT	-	1	-	-	1	1	-	-
B	-	7	-	-	-	-	-	-
NK	-	3	-	-	1	1	-	-
DCs	-	2	-	-	1	-	-	-
Monocytes	-	3	-	-	3	-	-	-
Signal: pSTAT5 (n=27, 24%)								
	US	IFN-α	IL-6	IL-7	IL-10	IL-21	LPS	PMA / Ionomycin
Basophils	-	-	-	-	-	-	-	-

$CD4^{+}T$	-	7	1	7	-	-	-	-
$CD8^{+}T$	-	6	-	4	-	-	-	-
$CD4^{-}CD8^{-}T$	-	-	-	-	-	-	-	-
$CD4^{+}CD8^{+}T$	-	-	-	1	-	-	-	-
NKT	-	-	-	1	-	-	-	-
B	-	-	-	-	-	-	-	-
NK	-	-	-	-	-	-	-	-
DCs	-	-	-	-	-	-	-	-
Monocytes	-	-	-	-	-	-	-	-
Signal: pPLCγ2 (n=4, 4%)								
	US	IFN-α	IL-6	IL-7	IL-10	IL-21	LPS	PMA / Ionomycin
All	-	-	-	1	1	1	-	1
Signal: pCREB (n=3, 3%)								
	US	IFN-α	IL-6	IL-7	IL-10	IL-21	LPS	PMA / Ionomycin
All	1	1	-	-	-	-	-	1
Signal: pSTAT3 (n=2, 2%)								
	US	IFN-α	IL-6	IL-7	IL-10	IL-21	LPS	PMA / Ionomycin
All	-	2	-	-	-	-	-	-
Signal: IκBα (n=1, 1%)								
	US	IFN-α	IL-6	IL-7	IL-10	IL-21	LPS	PMA / Ionomycin
All	-	-	-	1	-	-	-	-
Signal: p38 (n=1, 1%)								
	US	IFN-α	IL-6	IL-7	IL-10	IL-21	LPS	PMA / Ionomycin
All	-	-	-	-	-	-	-	1
Cluster 18 (n=289)								
Signal: pPLCγ2 (n=262, 91%)								
	US	IFN-α	IL-6	IL-7	IL-10	IL-21	LPS	PMA / Ionomycin
Basophils	-	-	-	-	-	-	-	-
$CD4^{+}T$	7	7	7	7	7	7	7	7
$CD8^{+}T$	6	6	6	6	6	6	6	6
$CD4^{-}CD8^{-}T$	1	1	1	1	1	1	1	1

$CD4^+CD8^+T$	1	1	1	1	1	1	1	1
NKT	1	1	1	1	1	1	1	1
B	8	7	8	8	8	8	8	7
NK	3	3	3	3	3	3	3	3
DCs	3	3	3	3	3	3	3	3
Monocytes	3	3	3	3	3	3	3	3
Signals: pS6 (n=14, 5%)								
	US	IFN-α	IL-6	IL-7	IL-10	IL-21	LPS	PMA / Ionomycin
All	1	2	2	1	2	1	3	2
Signal: pSTAT3 (n=5, 2%)								
	US	IFN-α	IL-6	IL-7	IL-10	IL-21	LPS	PMA / Ionomycin
All	-	2	-	-	3	-	-	-
Signal: pSTAT5 (n=3, 1%)								
	US	IFN-α	IL-6	IL-7	IL-10	IL-21	LPS	PMA / Ionomycin
All	-	3	-	-	-	-	-	-
Signal: pSTAT1 (n=3, 1%)								
	US	IFN-α	IL-6	IL-7	IL-10	IL-21	LPS	PMA / Ionomycin
All	-	1	-	-	2	-	-	-
Signal: IκBα (n=2, 1%)								
	US	IFN-α	IL-6	IL-7	IL-10	IL-21	LPS	PMA / Ionomycin
All	-	1	1	-	-	-	-	-

Cluster 19 (n=71)

Signal: pS6 (n=71, 100%)								
	US	IFN-α	IL-6	IL-7	IL-10	IL-21	LPS	PMA / Ionomycin
Basophils	-	-	-	-	-	-	-	-
$CD4^+T$	-	-	-	-	-	-	-	-
$CD8^+T$	-	-	-	-	-	-	-	-
$CD4^-CD8^-T$	-	-	-	-	-	-	-	-
$CD4^+CD8^+T$	-	-	-	-	-	-	-	-
NKT	-	-	-	-	-	-	-	-
B	8	7	8	7	8	8	8	-

NK	-	-	-	-	-	-	-	-
DCs	1	-	-	1	-	1	-	-
Monocytes	2	2	2	2	2	2	2	-
Cluster 20 (n=169)								
Signal: pSTAT1 (n=76, 45%)								
	US	IFN-α	IL-6	IL-7	IL-10	IL-21	LPS	PMA / Ionomycin
Basophils	-	1	1	-	1	1	-	-
$CD4^+T$	3	-	1	-	-	-	-	2
$CD8^+T$	-	-	3	-	-	-	-	-
$CD4^-CD8^-T$	-	-	-	-	-	-	-	-
$CD4^+CD8^+T$	1	-	1	-	-	-	-	-
NKT	-	-	1	-	-	-	-	-
B	8	1	7	8	-	-	7	7
NK	4	1	4	4	-	1	4	4
DCs	-	-	-	-	-	-	-	-
Monocytes	-	-	-	-	-	-	-	-
Signal: pSTAT3 (n=61, 36%)								
	US	IFN-α	IL-6	IL-7	IL-10	IL-21	LPS	PMA / Ionomycin
Basophils	-	-	-	-	-	-	-	-
$CD4^+T$	2	-	-	5	-	-	7	6
$CD8^+T$	-	-	2	-	-	-	1	1
$CD4^-CD8^-T$	-	-	-	-	-	-	-	-
$CD4^+CD8^+T$	-	-	1	-	-	-	-	-
NKT	-	-	1	-	-	-	-	-
B	3	1	2	2	-	5	8	8
NK	1	-	1	1	-	-	1	1
DCs	-	-	-	-	-	1	-	-
Monocytes	-	-	-	-	-	-	-	-
Signal: pPLCγ2 (n=14, 8%)								
	US	IFN-α	IL-6	IL-7	IL-10	IL-21	LPS	PMA / Ionomycin
All	2	3	2	1	1	1	2	2
Signal: pSTAT5 (n=9, 5%)								

	US	IFN-α	IL-6	IL-7	IL-10	IL-21	LPS	PMA / Ionomycin
All	-	3	1	4	1	-	-	-
Signal: pAKT (n=3, 2%)								
	US	IFN-α	IL-6	IL-7	IL-10	IL-21	LPS	PMA / Ionomycin
All	-	1	-	1	-	-	-	1
Signal: ERK-1/2 (n=3, 2%)								
	US	IFN-α	IL-6	IL-7	IL-10	IL-21	LPS	PMA / Ionomycin
All	-	-	-	-	-	-	3	-
Signal: pS6 (n=2, 1%)								
	US	IFN-α	IL-6	IL-7	IL-10	IL-21	LPS	PMA / Ionomycin
All	-	1	-	1	-	-	-	-
Signal: IκBα (n=1, 1%)								
	US	IFN-α	IL-6	IL-7	IL-10	IL-21	LPS	PMA / Ionomycin
All	-	-	-	-	-	-	-	1

Cluster 21 (n=147)

Signal: pS6 (n=146, 99%)								
	US	IFN-α	IL-6	IL-7	IL-10	IL-21	LPS	PMA / Ionomycin
Basophils	-	-	-	-	-	-	-	-
$CD4^{+}T$	7	7	7	7	7	7	7	-
$CD8^{+}T$	6	6	6	6	6	6	6	-
$CD4^{-}CD8^{-}T$	1	1	1	1	1	1	1	-
$CD4^{+}CD8^{+}T$	1	1	1	1	1	1	1	-
NKT	1	1	1	1	1	1	1	-
B	-	-	-	-	-	-	-	-
NK	4	4	4	4	4	4	4	-
DCs	-	-	-	-	-	-	-	-
Monocytes	1	1	1	1	1	1	-	-
Signal: IκBα (n=1, 1%)								
	US	IFN-α	IL-6	IL-7	IL-10	IL-21	LPS	PMA / Ionomycin
All	-	-	-	-	-	-	1	-

Cluster 22 (n=139)								
Signal: pAKT (n=139, 100%)								
	US	IFN-α	IL-6	IL-7	IL-10	IL-21	LPS	PMA / Ionomycin
Basophils	-	-	-	-	1	1	1	1
$CD4^+T$	-	-	-	-	7	7	7	7
$CD8^+T$	-	-	-	-	6	6	6	6
$CD4^-CD8^-T$	-	-	-	-	1	1	1	1
$CD4^+CD8^+T$	-	-	-	-	1	1	1	1
NKT	-	-	-	-	1	1	1	1
B	-	-	-	-	8	8	8	7
NK	-	-	-	-	4	4	4	4
DCs	-	-	-	-	3	3	3	3
Monocytes	-	-	-	-	3	3	3	3

Cluster 23 (n=140)								
Signal: EEA1 (n=140, 100%)								
	US	IFN-α	IL-6	IL-7	IL-10	IL-21	LPS	PMA / Ionomycin
Basophils	-	-	-	-	1	1	1	1
$CD4^+T$	-	-	-	-	7	7	7	7
$CD8^+T$	-	-	-	-	6	6	6	6
$CD4^-CD8^-T$	-	-	-	-	1	1	1	1
$CD4^+CD8^+T$	-	-	-	-	1	1	1	1
NKT	-	-	-	-	1	1	1	1
B	-	-	-	-	8	8	8	8
NK	-	-	-	-	4	4	4	4
DCs	-	-	-	-	3	3	3	3
Monocytes	-	-	-	-	3	3	3	3

Cluster 24 (n=275)								
Signal: pSTAT5 (n=137, 50%)								
	US	IFN-α	IL-6	IL-7	IL-10	IL-21	LPS	PMA / Ionomycin
Basophils	-	-	-	-	1	1	1	1
$CD4^+T$	-	-	-	-	6	6	7	7
$CD8^+T$	-	-	-	-	6	6	6	6

$CD4^{-}CD8^{-}T$	-	-	-	-	1	1	1	1
$CD4^{+}CD8^{+}T$	-	-	-	-	1	1	1	1
NKT	-	-	-	-	1	1	1	1
B	-	-	-	-	8	8	8	8
NK	-	-	-	-	4	4	4	4
DCs	-	-	-	-	2	3	3	3
Monocytes	-	-	-	-	3	3	3	3
Signal: p38 (n=95, 35%)								
	US	IFN-α	IL-6	IL-7	IL-10	IL-21	LPS	PMA / Ionomycin
Basophils	-	-	-	-	1	1	1	-
$CD4^{+}T$	-	-	-	-	7	7	7	-
$CD8^{+}T$	-	-	-	-	6	6	6	-
$CD4^{-}CD8^{-}T$	-	-	-	-	1	1	1	-
$CD4^{+}CD8^{+}T$	-	-	-	-	1	1	1	-
NKT	-	-	-	-	1	1	1	-
B	-	-	-	-	8	8	8	-
NK	-	-	-	-	4	4	4	-
DCs	-	-	-	-	2	2	2	-
Monocytes	-	-	-	-	1	1	-	-
Signal: pSTAT3 (n=43, 16%)								
	US	IFN-α	IL-6	IL-7	IL-10	IL-21	LPS	PMA / Ionomycin
Basophils	-	-	-	-	1	1	1	1
$CD4^{+}T$	-	-	-	-	-	-	-	1
$CD8^{+}T$	-	-	-	-	-	-	5	5
$CD4^{-}CD8^{-}T$	-	-	-	-	-	-	1	1
$CD4^{+}CD8^{+}T$	-	-	-	-	-	-	1	1
NKT	-	-	-	-	-	-	1	1
B	-	-	-	-	-	-	-	-
NK	-	-	-	-	-	-	3	3
DCs	-	-	-	-	-	2	3	3
Monocytes	-	-	-	-	-	2	3	3

Table S2. Demographics (age, sex, and number of *APOE* ε4 alleles) of participants in the discovery cohort by diagnostic group. Abbreviations*:* HC-I = Healthy Controls-I; AD = Alzheimer's disease; PD = Parkinson's disease; HC-II = Healthy Controls-II. Italicized HC-I samples are also HC-I_{sub}.

HC-I (n=53)			**AD** (n=28)			**PD** (n=17)			**HC-II** (n=10)		
Age	**Sex**	**#ε4**	**Age**	**Sex**	**#ε4**	**Age**	**Sex**	**#ε4**	**Age**	**Sex**	**#ε4**
67	*F*	*0*	*55*	*F*	1	67	F	1	31	F	NA
67	*F*	*0*	*57*	*F*	1	67	F	0	33	F	NA
69	*F*	*0*	*58*	*F*	NA	71	F	0	36	F	NA
69	*F*	*0*	*59*	*F*	0	72	F	0	37	F	NA
70	*F*	*1*	*61*	*F*	0	74	F	0	42	F	NA
71	*F*	*0*	*61*	*F*	NA	75	F	0	58	F	NA
71	*F*	*1*	*62*	*F*	1	63	M	0	32	M	NA
71	*F*	*0*	*64*	*F*	NA	65	M	1	33	M	NA
72	*F*	*0*	*70*	*F*	1	67	M	0	45	M	NA
73	*F*	*0*	*70*	*F*	1	67	M	1	48	M	NA
73	*F*	*0*	*71*	*F*	NA	68	M	0			
73	*F*	*0*	*76*	*F*	1	68	M	0			
63	*M*	*NA*	*83*	*F*	1	70	M	0			
65	*M*	*0*	84	F	1	73	M	0			
67	*M*	*0*	60	M	1	75	M	0			
68	*M*	*0*	61	M	0	77	M	0			
68	*M*	*0*	62	M	2	78	M	0			

69	*M*	*0*	62	M	1
69	*M*	*NA*	69	M	0
70	*M*	*NA*	70	M	2
72	*M*	*1*	75	M	NA
72	*M*	*0*	78	M	NA
73	*M*	*0*	80	M	0
73	*M*	*0*	81	M	NA
74	*M*	*0*	83	M	1
74	*M*	*0*	83	M	1
75	*M*	*0*	83	M	0
76	*M*	*0*	87	M	0
78	*M*	*1*			
78	*M*	*1*			
78	*M*	*NA*			
80	*M*	*1*			
80	*M*	*0*			
80	*M*	*0*			
59	F	NA			
59	F	NA			
59	F	NA			
61	F	NA			
62	F	0			
62	F	NA			

63	F	0	
64	F	1	
66	F	0	
76	F	NA	
79	F	0	
80	F	0	
55	M	NA	
81	M	0	
82	M	2	
83	M	0	
84	M	0	
87	M	1	
94	M	0	

Table S3. Demographics (age, sex, and number of *APOE* ε4 alleles) of participants in the validation cohort by diagnostic group. HC-V = Healthy controls validation; AD-V = Alzheimer's disease validation.

HC-V (n=15)			**AD-V** (n=9)		
Age	**Sex**	**# ε4**	**Age**	**Sex**	**# ε4**
62	F	NA	60	F	NA
63	F	NA	63	F	NA
67	F	1	70	F	NA
67	F	NA	81	F	0
70	F	0	81	F	NA
70	F	0	65	M	0
73	F	NA	70	M	NA
78	F	0	86	M	0
80	F	2	91	M	NA
61	M	1			
64	M	0			
66	M	1			
69	M	2			
77	M	0			
89	M	0			

Table S4. Target, clone, and conjugation information and product identifier.				
Metal	**Target**	**Clone**	**Conjugation**	**Product identifier**
113 In	Rab5	SC-28570	In House	Santa Cruz Cat # sc28570
115 In	Lamp2	H4B4	In House	Biolegend Cat# 354302
140 Ce	Beads	NA	NA	Fluidigm Cat # 201078
142 Nd	EEA1	C45B10	In House	Cell signaling Cat # 3288BF
143 Nd	CD19	HIB19	In House	Biolegend Cat # 302202
144 Nd	pPLCγ2	K86-689.37	Fluidigm	Fluidigm Cat # 3144015A
145 Nd	CD4	RPA-T4	Fluidigm	Fluidigm Cat # 3145001B
146 Nd	IgD	IA6-2	Fluidigm	Fluidigm Cat # 3146005B
147 Sm	CD20	H1	In House	BD Cat # 555677
148 Nd	IgA	Polyclonal	Fluidigm	Fluidigm Cat # 3148007B
149 Sm	CD25	2A3	Fluidigm	Fluidigm Cat # 3149010B
150 Nd	pSTAT5	47	Fluidigm	Fluidigm Cat # 3150005A
151 Eu	CD123	6H6	Fluidigm	Fluidigm Cat # 3151001B
152 Sm	pAKT	D9E	Fluidigm	Fluidigm Cat # 3152005A
153 Eu	pSTAT1	4a	Fluidigm	Fluidigm Cat # 3153005A
154 Sm	CD27	O323	In house	Biolegend Cat # 302802
156 Gd	p38	D3F9	Fluidigm	Fluidigm Cat # 3156002A
157 Gd	CD24	ML-5	In House	Biolegend Cat # 555246
158 Gd	pSTAT3	4	Fluidigm	Fluidigm Cat # 3158005A
159 Tb	CD11c	Bu15	Fluidigm	Fluidigm Cat # 3159001B
160 Gd	CD14	M5E2	Fluidigm	Fluidigm Cat # 3160001B

162 Dy	pLCK	4/LCK-Y505	Fluidigm	Fluidigm Cat # 3162004A
163 Dy	CD56	NCAM16.2	Fluidigm	Fluidigm Cat # 3163007B
164 Dy	IκBα	L35A5	Fluidigm	Fluidigm Cat # 3164004A
165 Ho	pCREB	87G3	Fluidigm	Fluidigm Cat # 3165009A
166 Er	CD16	B73.1	In House	Ebioscience Cat # 16-0167-85
167 Er	CD38	HIT2	Fluidigm	Fluidigm Cat # 3167001B
168 Er	CD8	SK1	Fluidigm	Fluidigm Cat # 3168002B
169 Tm	CD45RA	HI100	Fluidigm	Fluidigm Cat # 3169008B
170 Er	CD3	UCHT1	Fluidigm	Fluidigm Cat # 3170001B
171 Yb	pERK1/2	D13.14.4E	Fluidigm	Fluidigm Cat # 3171010A
172 Yb	NF-κB	4D1	In House	Biolegend Cat # 616702
173 Yb	CD7	CD7-6B7	in House	Biolegend Cat # 343102
174 Yb	HLA-DR	L243	Fluidigm	Fluidigm Cat # 3174001B
175 Lu	pS6	N7-548	Fluidigm	Fluidigm Cat # 3175009A
176 Yb	CD127	AO19D5	Fluidigm	Fluidigm Cat # 3176004B
209 Bi	CD11b	ICRF44	Fluidigm	Fluidigm Cat # 3209003B

Table S5. Stimulants used to activate PBMCs.

Stimulation	Source	Catalog #	Final Concentration
IFN-α	PBL Interferon Source	11105-1	10,000 units/ml
IL-6	BD Biosciences	550071	50 ng/ml
IL-7	BD Biosciences	554608	50 ng/ml
IL-10	BD Biosciences	554611	50 ng/ml
IL-21	Life Sciences, Gibco	PHC0214	50 ng/ml
LPS	Sigma-Aldrich	L7770	1 μg/ml
PMA	Sigma-Aldrich	P8139	100 ng /ml
Ionomycin	Calbiochem	407952	1000 ng/ml

Table S6. Cell counts for each stimulating condition in each gated population. Data are aggregated over all 132 samples after collecting over 1.2 million events, removing unassigned events, and subsampling at a maximum of 100,000 per sample. Cell type hierarchy is shown in the gating strategy in Figs. S9 and S10. Non BT = non B and T cell populations. US = unstimulated.

Cell Type	US	IFN-α	IL-6	IL-7	IL-10	IL-21	LPS	PMA / ionomycin
Total	10395247	9211105	9489772	9702098	9677665	9501021	9290856	6299873
Basophils	66653	58688	56805	61943	57009	58859	59631	47100
Non-Basophils	10328219	9152166	9432369	9640722	9601849	9442604	9231008	6253340
Lymphocytes	9095101	8045968	8325915	8507811	8476132	8319355	8417538	5894545
$CD3^+$	5552179	5346089	5544292	5664958	5693952	5551715	5662085	3980790
$CD4^+$ T	3627601	3605486	3714372	3799720	3837919	3735140	3790062	2737586
$CD4^+$ $T_{Activated}$	126924	82531	96166	92021	82700	185979	160110	74966
$CD4^+$ $T_{Central\ mem}$	1309750	1103655	1298995	967176	1297499	1322305	1297210	855152
$CD4^+$ $T_{Effector}$	409931	566536	437759	768720	482418	423783	466230	390825
$CD4^+$ $T_{Effector\ mem}$	749178	986458	844018	1145457	852060	793195	852455	616625
$CD4^+$ T_{Naive}	1179982	948837	1133600	870036	1205942	1195857	1174167	874984
Tregs	131887	171258	146641	190470	103427	114381	140269	90748
$CD4^+CD8^+$ T	35710	29399	24980	27205	40345	33213	30300	19139
$CD4^-CD8^-$ T	464100	339988	463239	424230	371336	386132	416981	312066
$CD8^+$ T	1388762	1350354	1392099	1426058	1427799	1398490	1413784	922034
$CD8^+$ $T_{Activated}$	64575	43528	45927	49380	60235	66249	71182	38411
$CD8^+$ $T_{Central\ mem}$	345435	318163	338020	260518	401047	346902	337211	193823
$CD8^+$ $T_{Effector}$	335817	304559	335531	350787	267044	327134	313318	247808
$CD8^+$ $T_{Effector\ mem}$	300537	436033	304434	560383	434606	303298	352605	206625
$CD8^+$ T_{Naive}	406973	291599	414114	254370	325102	421156	410650	273778
NKT	552568	644955	858632	1570626	320470	480082	458057	302114

$CD3^-$	2878194	2276246	2327506	2574372	2583485	2514451	2531164	1751016
B	676242	781732	758498	675728	690728	680787	708495	487435
IgA^+ B	40532	37705	36804	37600	32385	39269	39834	25222
IgD^+ B_{mem}	185183	167942	167799	201120	175032	195696	188687	131176
IgD^- $CD27^-$ B	132963	112299	121480	114681	140874	119299	131640	90951
B_{Naive}	248728	288504	242719	279299	282697	281380	301257	209709
Plasmablast	30653	13553	68474	15791	29412	31762	31750	15845
$B_{Switched\ mem}$	109368	69480	82993	80628	92125	84412	86911	55599
$B_{Transitional}$	40882	40740	86892	49629	33890	38326	40368	40883
$CD3^-$, Non BT	2196571	1777051	1843924	1888413	1885181	1825506	1815090	1258690
NK	1132857	1015775	1029519	1049397	1065365	1025886	1068659	771655
$CD16^{high}$ NK	720283	614177	709463	713457	740438	720555	729661	409562
$CD56^{bright}$ NK	129606	150824	97999	96871	89095	90876	89071	61607
$CD56^{dim}$ $CD16^{dim}$ NK	242878	236543	190472	229071	223467	200150	225960	281472
DCs	1019121	749922	783600	813479	796195	774080	725795	471444
mDCs	470477	398511	408850	437272	434655	441499	399322	247880
pDCs	31464	30669	30579	32575	34276	33665	32537	17384
Mono	1225245	1098538	1100431	1123949	1118209	1115297	806898	354578
$CD16^{high}$ Mono	214399	172410	117624	87052	139313	237922	87240	73242
$CD16^{low}$ Mono	1003228	919005	977516	1032601	967969	867290	715020	283842

Table S7. Prioritization matrix used for iEN model (1 indicates canonical response).

Cell Type (Unstimulated)	Lamp2	Rab5	EEA1	pSTAT1	pSTAT3	pSTAT5	pPLCγ2	pAKT	p38	pLCK	Ikba	pCREB	pERK1/2	NFkB	pS6
Basophils	1	1	1	1	1	1	1	1	1	1	1	1	1	1	1
CD4$^+$ T	1	1	1	1	1	1	1	1	1	1	1	1	1	1	1
CD4$^+$ T$_{Activated}$	1	1	1	1	1	1	1	1	1	1	1	1	1	1	1
CD4$^+$ T$_{Central\ mem}$	1	1	1	1	1	1	1	1	1	1	1	1	1	1	1
CD4$^+$ T$_{Effector}$	1	1	1	1	1	1	1	1	1	1	1	1	1	1	1
CD4$^+$ T$_{Effector\ mem}$	1	1	1	1	1	1	1	1	1	1	1	1	1	1	1
CD4$^+$ T$_{Naïve}$	1	1	1	1	1	1	1	1	1	1	1	1	1	1	1
Tregs	1	1	1	1	1	1	1	1	1	1	1	1	1	1	1
CD8$^+$ T	1	1	1	1	1	1	1	1	1	1	1	1	1	1	1
CD8$^+$ T$_{Activated}$	1	1	1	1	1	1	1	1	1	1	1	1	1	1	1
CD8$^+$ T$_{Central\ mem}$	1	1	1	1	1	1	1	1	1	1	1	1	1	1	1
CD8$^+$ T$_{Effector}$	1	1	1	1	1	1	1	1	1	1	1	1	1	1	1
CD8$^+$ T$_{Effector\ mem}$	1	1	1	1	1	1	1	1	1	1	1	1	1	1	1
CD8$^+$ T$_{Naïve}$	1	1	1	1	1	1	1	1	1	1	1	1	1	1	1
B	1	1	1	1	1	1	1	1	1	1	1	1	1	1	1
IgA$^+$ B	1	1	1	1	1	1	1	1	1	1	1	1	1	1	1
IgD$^+$ B$_{mem}$	1	1	1	1	1	1	1	1	1	1	1	1	1	1	1
IgD$^-$CD27$^-$ B	1	1	1	1	1	1	1	1	1	1	1	1	1	1	1
B$_{Naïve}$	1	1	1	1	1	1	1	1	1	1	1	1	1	1	1
Plasmablast	1	1	1	1	1	1	1	1	1	1	1	1	1	1	1
B$_{Switched\ mem}$	1	1	1	1	1	1	1	1	1	1	1	1	1	1	1
B$_{Transitional}$	1	1	1	1	1	1	1	1	1	1	1	1	1	1	1
DCs	1	1	1	1	1	1	1	1	1	1	1	1	1	1	1
mDCs	1	1	1	1	1	1	1	1	1	1	1	1	1	1	1
pDCs	1	1	1	1	1	1	1	1	1	1	1	1	1	1	1
NK	1	1	1	1	1	1	1	1	1	1	1	1	1	1	1
CD16^{high} NK	1	1	1	1	1	1	1	1	1	1	1	1	1	1	1
CD56^{bright} NK	1	1	1	1	1	1	1	1	1	1	1	1	1	1	1
CD56^{dim}CD16^{dim} NK	1	1	1	1	1	1	1	1	1	1	1	1	1	1	1

NKT	1	1	1	1	1	1	1	1	1	1	1	1	1	1	1
Mono	1	1	1	1	1	1	1	1	1	1	1	1	1	1	1
CD16^{low} Mono	1	1	1	1	1	1	1	1	1	1	1	1	1	1	1
CD16^{high} Mono	1	1	1	1	1	1	1	1	1	1	1	1	1	1	1

Cell Type (IFN-α)	**Lamp2**	**Rab5**	**EEA1**	**pSTAT1**	**pSTAT3**	**pSTAT5**	**pPLCγ2**	**pAKT**	**p38**	**pLCK**	**Ikba**	**pCREB**	**pERK1/2**	**NFkB**	**pS6**
Basophils	0	0	0	1	1	1	0	0	0	0	0	0	0	0	0
CD4^{+} T	0	0	0	1	1	1	0	0	0	0	0	0	0	0	0
CD4^{+} T$_{Activated}$	0	0	0	1	1	1	0	0	0	0	0	0	0	0	0
CD4^{+} T$_{Central\ mem}$	0	0	0	1	1	1	0	0	0	0	0	0	0	0	0
CD4^{+} T$_{Effector}$	0	0	0	1	1	1	0	0	0	0	0	0	0	0	0
CD4^{+} T$_{Effector\ mem}$	0	0	0	1	1	1	0	0	0	0	0	0	0	0	0
CD4^{+} T$_{Naïve}$	0	0	0	1	1	1	0	0	0	0	0	0	0	0	0
Tregs	0	0	0	1	1	1	0	0	0	0	0	0	0	0	0
CD8^{+} T	0	0	0	1	1	1	0	0	0	0	0	0	0	0	0
CD8^{+} T$_{Activated}$	0	0	0	1	1	1	0	0	0	0	0	0	0	0	0
CD8^{+} T$_{Central\ mem}$	0	0	0	1	1	1	0	0	0	0	0	0	0	0	0
CD8^{+} T$_{Effector}$	0	0	0	1	1	1	0	0	0	0	0	0	0	0	0
CD8^{+} T$_{Effector\ mem}$	0	0	0	1	1	1	0	0	0	0	0	0	0	0	0
CD8^{+} T$_{Naïve}$	0	0	0	1	1	1	0	0	0	0	0	0	0	0	0
B	0	0	0	1	1	1	0	0	0	0	0	0	0	0	0
IgA^{+} B	0	0	0	1	1	1	0	0	0	0	0	0	0	0	0
IgD^{+} B$_{mem}$	0	0	0	1	1	1	0	0	0	0	0	0	0	0	0
IgD^{-}CD27^{-} B	0	0	0	1	1	1	0	0	0	0	0	0	0	0	0
B$_{Naïve}$	0	0	0	1	1	1	0	0	0	0	0	0	0	0	0
Plasmablast	0	0	0	1	1	1	0	0	0	0	0	0	0	0	0
B$_{Switched\ mem}$	0	0	0	1	1	1	0	0	0	0	0	0	0	0	0
B$_{Transitional}$	0	0	0	1	1	1	0	0	0	0	0	0	0	0	0
DCs	0	0	0	1	1	1	0	0	0	0	0	0	0	0	0
mDCs	0	0	0	1	1	1	0	0	0	0	0	0	0	0	0
pDCs	0	0	0	1	1	1	0	0	0	0	0	0	0	0	0
NK	0	0	0	1	1	1	0	0	0	0	0	0	0	0	0
CD16^{high} NK	0	0	0	1	1	1	0	0	0	0	0	0	0	0	0

CD56^{bright} NK	0	0	0	1	1	1	0	0	0	0	0	0	0	0	0
CD56^{dim}CD16^{dim} NK	0	0	0	1	1	1	0	0	0	0	0	0	0	0	0
NKT	0	0	0	1	1	1	0	0	0	0	0	0	0	0	0
Mono	0	0	0	1	1	1	0	0	0	0	0	0	0	0	0
CD16^{low} Mono	0	0	0	1	1	1	0	0	0	0	0	0	0	0	0
CD16^{high} Mono	0	0	0	1	1	1	0	0	0	0	0	0	0	0	0

Cell Type (IL-6)	**Lamp2**	**Rab5**	**EEA1**	**pSTAT1**	**pSTAT3**	**pSTAT5**	**pPLCγ2**	**pAKT**	**p38**	**pLCK**	**Ikba**	**pCREB**	**pERK1/2**	**NFkB**	**pS6**
Basophils	0	0	0	1	1	1	0	0	0	0	0	0	1	0	0
CD4^{+} T	0	0	0	1	1	1	0	0	0	0	0	0	1	0	0
CD4^{+} T$_{Activated}$	0	0	0	1	1	1	0	0	0	0	0	0	1	0	0
CD4^{+} T$_{Central\ mem}$	0	0	0	1	1	1	0	0	0	0	0	0	1	0	0
CD4^{+} T$_{Effector}$	0	0	0	1	1	1	0	0	0	0	0	0	1	0	0
CD4^{+} T$_{Effector\ mem}$	0	0	0	1	1	1	0	0	0	0	0	0	1	0	0
CD4^{+} T$_{Naïve}$	0	0	0	1	1	1	0	0	0	0	0	0	1	0	0
Tregs	0	0	0	1	1	1	0	0	0	0	0	0	1	0	0
CD8^{+} T	0	0	0	1	1	1	0	0	0	0	0	0	1	0	0
CD8^{+} T$_{Activated}$	0	0	0	1	1	1	0	0	0	0	0	0	1	0	0
CD8^{+} T$_{Central\ mem}$	0	0	0	1	1	1	0	0	0	0	0	0	1	0	0
CD8^{+} T$_{Effector}$	0	0	0	1	1	1	0	0	0	0	0	0	1	0	0
CD8^{+} T$_{Effector\ mem}$	0	0	0	1	1	1	0	0	0	0	0	0	1	0	0
CD8^{+} T$_{Naïve}$	0	0	0	1	1	1	0	0	0	0	0	0	1	0	0
B	0	0	0	1	1	1	0	0	0	0	0	0	1	0	0
IgA^{+} B	0	0	0	1	1	1	0	0	0	0	0	0	1	0	0
IgD^{+} B$_{mem}$	0	0	0	1	1	1	0	0	0	0	0	0	1	0	0
IgD^{-}CD27^{-} B	0	0	0	1	1	1	0	0	0	0	0	0	1	0	0
B$_{Naïve}$	0	0	0	1	1	1	0	0	0	0	0	0	1	0	0
Plasmablast	0	0	0	1	1	1	0	0	0	0	0	0	1	0	0
B$_{Switched\ mem}$	0	0	0	1	1	1	0	0	0	0	0	0	1	0	0
B$_{Transitional}$	0	0	0	1	1	1	0	0	0	0	0	0	1	0	0
DCs	0	0	0	1	1	1	0	0	0	0	0	0	1	0	0
mDCs	0	0	0	1	1	1	0	0	0	0	0	0	1	0	0
pDCs	0	0	0	1	1	1	0	0	0	0	0	0	1	0	0

NK	0	0	0	1	1	1	0	0	0	0	0	0	1	0	0
CD16^{high} NK	0	0	0	1	1	1	0	0	0	0	0	0	1	0	0
CD56^{bright} NK	0	0	0	1	1	1	0	0	0	0	0	0	1	0	0
CD56^{dim}CD16^{dim} NK	0	0	0	1	1	1	0	0	0	0	0	0	1	0	0
NKT	0	0	0	1	1	1	0	0	0	0	0	0	1	0	0
Mono	0	0	0	1	1	1	0	0	0	0	0	0	1	0	0
CD16^{low} Mono	0	0	0	1	1	1	0	0	0	0	0	0	1	0	0
CD16^{high} Mono	0	0	0	1	1	1	0	0	0	0	0	0	1	0	0
Cell Type (IL-7)	**Lamp2**	**Rab5**	**EEA1**	**pSTAT1**	**pSTAT3**	**pSTAT5**	**pPLCγ2**	**pAKT**	**p38**	**pLCK**	**Ikba**	**pCREB**	**pERK1/2**	**NFkB**	**pS6**
Basophils	0	0	0	1	0	1	0	0	0	0	0	0	0	0	0
CD4^{+} T	0	0	0	1	0	1	0	0	0	0	0	0	0	0	0
CD4^{+} T$_{Activated}$	0	0	0	1	0	1	0	0	0	0	0	0	0	0	0
CD4^{+} T$_{Central\ mem}$	0	0	0	1	0	1	0	0	0	0	0	0	0	0	0
CD4^{+} T$_{Effector}$	0	0	0	1	0	1	0	0	0	0	0	0	0	0	0
CD4^{+} T$_{Effector\ mem}$	0	0	0	1	0	1	0	0	0	0	0	0	0	0	0
CD4^{+} T$_{Naïve}$	0	0	0	1	0	1	0	0	0	0	0	0	0	0	0
Tregs	0	0	0	1	0	1	0	0	0	0	0	0	0	0	0
CD8^{+} T	0	0	0	1	0	1	0	0	0	0	0	0	0	0	0
CD8^{+} T$_{Activated}$	0	0	0	1	0	1	0	0	0	0	0	0	0	0	0
CD8^{+} T$_{Central\ mem}$	0	0	0	1	0	1	0	0	0	0	0	0	0	0	0
CD8^{+} T$_{Effector}$	0	0	0	1	0	1	0	0	0	0	0	0	0	0	0
CD8^{+} T$_{Effector\ mem}$	0	0	0	1	0	1	0	0	0	0	0	0	0	0	0
CD8^{+} T$_{Naïve}$	0	0	0	1	0	1	0	0	0	0	0	0	0	0	0
B	0	0	0	0	0	0	0	0	0	0	0	0	0	0	0
IgA^{+} B	0	0	0	0	0	0	0	0	0	0	0	0	0	0	0
IgD^{+} B$_{mem}$	0	0	0	0	0	0	0	0	0	0	0	0	0	0	0
IgD^{-}CD27^{-} B	0	0	0	0	0	0	0	0	0	0	0	0	0	0	0
B$_{Naïve}$	0	0	0	0	0	0	0	0	0	0	0	0	0	0	0
Plasmablast	0	0	0	0	0	0	0	0	0	0	0	0	0	0	0
B$_{Switched\ mem}$	0	0	0	0	0	0	0	0	0	0	0	0	0	0	0
B$_{Transitional}$	0	0	0	0	0	0	0	0	0	0	0	0	0	0	0
DCs	0	0	0	0	0	0	0	0	0	0	0	0	0	0	0

mDCs	0	0	0	0	0	0	0	0	0	0	0	0	0	0	0
pDCs	0	0	0	0	0	0	0	0	0	0	0	0	0	0	0
NK	0	0	0	0	0	0	0	0	0	0	0	0	0	0	0
CD16^{high} NK	0	0	0	0	0	0	0	0	0	0	0	0	0	0	0
CD56^{bright} NK	0	0	0	0	0	0	0	0	0	0	0	0	0	0	0
CD56^{dim}CD16^{dim} NK	0	0	0	0	0	0	0	0	0	0	0	0	0	0	0
NKT	0	0	0	0	0	0	0	0	0	0	0	0	0	0	0
Mono	0	0	0	0	0	0	0	0	0	0	0	0	0	0	0
CD16^{low} Mono	0	0	0	0	0	0	0	0	0	0	0	0	0	0	0
CD16^{high} Mono	0	0	0	0	0	0	0	0	0	0	0	0	0	0	0

Cell Type (IL-10)	Lamp2	Rab5	EEA1	pSTAT1	pSTAT3	pSTAT5	pPLCγ2	pAKT	p38	pLCK	Ikba	pCREB	pERK1/2	NFkB	pS6
Basophils	0	0	0	1	1	1	0	0	0	0	0	0	0	0	0
CD4^{+} T	0	0	0	1	1	1	0	0	0	0	0	0	0	0	0
CD4^{+} T$_{Activated}$	0	0	0	1	1	1	0	0	0	0	0	0	0	0	0
CD4^{+} T$_{Central\ mem}$	0	0	0	1	1	1	0	0	0	0	0	0	0	0	0
CD4^{+} T$_{Effector}$	0	0	0	1	1	1	0	0	0	0	0	0	0	0	0
CD4^{+} T$_{Effector\ mem}$	0	0	0	1	1	1	0	0	0	0	0	0	0	0	0
CD4^{+} T$_{Naïve}$	0	0	0	1	1	1	0	0	0	0	0	0	0	0	0
Tregs	0	0	0	1	1	1	0	0	0	0	0	0	0	0	0
CD8^{+} T	0	0	0	1	1	1	0	0	0	0	0	0	0	0	0
CD8^{+} T$_{Activated}$	0	0	0	1	1	1	0	0	0	0	0	0	0	0	0
CD8^{+} T$_{Central\ mem}$	0	0	0	1	1	1	0	0	0	0	0	0	0	0	0
CD8^{+} T$_{Effector}$	0	0	0	1	1	1	0	0	0	0	0	0	0	0	0
CD8^{+} T$_{Effector\ mem}$	0	0	0	1	1	1	0	0	0	0	0	0	0	0	0
CD8^{+} T$_{Naïve}$	0	0	0	1	1	1	0	0	0	0	0	0	0	0	0
B	0	0	0	1	1	1	0	0	0	0	0	0	0	0	0
IgA^{+} B	0	0	0	1	1	1	0	0	0	0	0	0	0	0	0
IgD^{+} B$_{mem}$	0	0	0	1	1	1	0	0	0	0	0	0	0	0	0
IgD^{-}CD27^{-} B	0	0	0	1	1	1	0	0	0	0	0	0	0	0	0
B$_{Naïve}$	0	0	0	1	1	1	0	0	0	0	0	0	0	0	0
Plasmablast	0	0	0	1	1	1	0	0	0	0	0	0	0	0	0
B$_{Switched\ mem}$	0	0	0	1	1	1	0	0	0	0	0	0	0	0	0

$B_{Transitional}$	0	0	0	1	1	1	0	0	0	0	0	0	0	0	0
DCs	0	0	0	1	1	1	0	0	0	0	0	0	0	0	0
mDCs	0	0	0	1	1	1	0	0	0	0	0	0	0	0	0
pDCs	0	0	0	1	1	1	0	0	0	0	0	0	0	0	0
NK	0	0	0	1	1	1	0	0	0	0	0	0	0	0	0
CD16^{high} NK	0	0	0	1	1	1	0	0	0	0	0	0	0	0	0
CD56^{bright} NK	0	0	0	1	1	1	0	0	0	0	0	0	0	0	0
CD56^{dim}CD16^{dim} NK	0	0	0	1	1	1	0	0	0	0	0	0	0	0	0
NKT	0	0	0	1	1	1	0	0	0	0	0	0	0	0	0
Mono	0	0	0	1	1	1	0	0	0	0	0	0	0	0	0
CD16^{low} Mono	0	0	0	1	1	1	0	0	0	0	0	0	0	0	0
CD16^{high} Mono	0	0	0	1	1	1	0	0	0	0	0	0	0	0	0

Cell Type (IL-21)	Lamp2	Rab5	EEA1	pSTAT1	pSTAT3	pSTAT5	pPLCγ2	pAKT	p38	pLCK	Ikba	pCREB	pERK1/2	NFkB	pS6
Basophils	0	0	0	1	1	1	0	0	0	0	0	0	0	0	0
CD4^{+} T	0	0	0	1	1	1	0	0	0	0	0	0	0	0	0
CD4^{+} $T_{Activated}$	0	0	0	1	1	1	0	0	0	0	0	0	0	0	0
CD4^{+} $T_{Central\ mem}$	0	0	0	1	1	1	0	0	0	0	0	0	0	0	0
CD4^{+} $T_{Effector}$	0	0	0	1	1	1	0	0	0	0	0	0	0	0	0
CD4^{+} $T_{Effector\ mem}$	0	0	0	1	1	1	0	0	0	0	0	0	0	0	0
CD4^{+} $T_{Naïve}$	0	0	0	1	1	1	0	0	0	0	0	0	0	0	0
Tregs	0	0	0	1	1	1	0	0	0	0	0	0	0	0	0
CD8^{+} T	0	0	0	1	1	1	0	0	0	0	0	0	0	0	0
CD8^{+} $T_{Activated}$	0	0	0	1	1	1	0	0	0	0	0	0	0	0	0
CD8^{+} $T_{Central\ mem}$	0	0	0	1	1	1	0	0	0	0	0	0	0	0	0
CD8^{+} $T_{Effector}$	0	0	0	1	1	1	0	0	0	0	0	0	0	0	0
CD8^{+} $T_{Effector\ mem}$	0	0	0	1	1	1	0	0	0	0	0	0	0	0	0
CD8^{+} $T_{Naïve}$	0	0	0	1	1	1	0	0	0	0	0	0	0	0	0
B	0	0	0	1	1	1	0	0	0	0	0	0	0	0	0
IgA^{+} B	0	0	0	1	1	1	0	0	0	0	0	0	0	0	0
IgD^{+} B_{mem}	0	0	0	1	1	1	0	0	0	0	0	0	0	0	0
IgD^{-}CD27^{-} B	0	0	0	1	1	1	0	0	0	0	0	0	0	0	0
$B_{Naïve}$	0	0	0	1	1	1	0	0	0	0	0	0	0	0	0

Plasmablast	0	0	0	1	1	1	0	0	0	0	0	0	0	0	0
B$_{Switched\ mem}$	0	0	0	1	1	1	0	0	0	0	0	0	0	0	0
B$_{Transitional}$	0	0	0	1	1	1	0	0	0	0	0	0	0	0	0
DCs	0	0	0	1	1	1	0	0	0	0	0	0	0	0	0
mDCs	0	0	0	1	1	1	0	0	0	0	0	0	0	0	0
pDCs	0	0	0	1	1	1	0	0	0	0	0	0	0	0	0
NK	0	0	0	1	1	1	0	0	0	0	0	0	0	0	0
CD16^{high} NK	0	0	0	1	1	1	0	0	0	0	0	0	0	0	0
CD56^{bright} NK	0	0	0	1	1	1	0	0	0	0	0	0	0	0	0
CD56^{dim}CD16^{dim} NK	0	0	0	1	1	1	0	0	0	0	0	0	0	0	0
NKT	0	0	0	1	1	1	0	0	0	0	0	0	0	0	0
Mono	0	0	0	1	1	1	0	0	0	0	0	0	0	0	0
CD16^{low} Mono	0	0	0	1	1	1	0	0	0	0	0	0	0	0	0
CD16^{high} Mono	0	0	0	1	1	1	0	0	0	0	0	0	0	0	0
Cell Type (LPS)	**Lamp2**	**Rab5**	**EEA1**	**pSTAT1**	**pSTAT3**	**pSTAT5**	**pPLCγ2**	**pAKT**	**p38**	**pLCK**	**Ikba**	**pCREB**	**pERK1/2**	**NFkB**	**pS6**
Basophils	0	0	0	0	0	0	0	0	0	0	0	0	0	0	0
CD4^{+} T	0	0	0	0	0	0	0	0	0	0	0	0	0	0	0
CD4^{+} T$_{Activated}$	0	0	0	0	0	0	0	0	0	0	0	0	0	0	0
CD4^{+} T$_{Central\ mem}$	0	0	0	0	0	0	0	0	0	0	0	0	0	0	0
CD4^{+} T$_{Effector}$	0	0	0	0	0	0	0	0	0	0	0	0	0	0	0
CD4^{+} T$_{Effector\ mem}$	0	0	0	0	0	0	0	0	0	0	0	0	0	0	0
CD4^{+} T$_{Naïve}$	0	0	0	0	0	0	0	0	0	0	0	0	0	0	0
Tregs	0	0	0	0	0	0	0	0	1	0	1	1	1	1	1
CD8^{+} T	0	0	0	0	0	0	0	0	0	0	0	0	0	0	0
CD8^{+} T$_{Activated}$	0	0	0	0	0	0	0	0	0	0	0	0	0	0	0
CD8^{+} T$_{Central\ mem}$	0	0	0	0	0	0	0	0	0	0	0	0	0	0	0
CD8^{+} T$_{Effector}$	0	0	0	0	0	0	0	0	0	0	0	0	0	0	0
CD8^{+} T$_{Effector\ mem}$	0	0	0	0	0	0	0	0	0	0	0	0	0	0	0
CD8^{+} T$_{Naïve}$	0	0	0	0	0	0	0	0	0	0	0	0	0	0	0
B	0	0	0	0	0	0	0	0	0	0	0	0	0	0	0
IgA^{+} B	0	0	0	0	0	0	0	0	0	0	0	0	0	0	0
IgD^{+} B$_{mem}$	0	0	0	0	0	0	0	0	0	0	0	0	0	0	0

IgD$^-$CD27$^-$ B	0	0	0	0	0	0	0	0	0	0	0	0	0	0	0
B$_{Naïve}$	0	0	0	0	0	0	0	0	0	0	0	0	0	0	0
Plasmablast	0	0	0	0	0	0	0	0	0	0	0	0	0	0	0
B$_{Switched\ mem}$	0	0	0	0	0	0	0	0	0	0	0	0	0	0	0
B$_{Transitional}$	0	0	0	0	0	0	0	0	0	0	0	0	0	0	0
DCs	0	0	0	0	0	0	0	0	0	0	0	0	0	0	0
mDCs	0	0	0	0	0	0	0	0	1	0	1	1	1	1	1
pDCs	0	0	0	0	0	0	0	0	0	0	0	0	0	0	0
NK	0	0	0	0	0	0	0	0	1	0	1	1	1	1	1
CD16^{high} NK	0	0	0	0	0	0	0	0	1	0	1	1	1	1	1
CD56^{bright} NK	0	0	0	0	0	0	0	0	1	0	1	1	1	1	1
CD56^{dim}CD16^{dim} NK	0	0	0	0	0	0	0	0	1	0	1	1	1	1	1
NKT	0	0	0	0	0	0	0	0	1	0	1	1	1	1	1
Mono	0	0	0	0	0	0	0	0	0	0	0	0	0	0	0
CD16^{low} Mono	0	0	0	0	0	0	0	0	0	0	0	0	0	0	0
CD16^{high} Mono	0	0	0	0	0	0	0	0	0	0	0	0	0	0	0
Cell Type (PMA/ionomycin)	**Lamp2**	**Rab5**	**EEA1**	**pSTAT1**	**pSTAT3**	**pSTAT5**	**pPLCγ2**	**pAKT**	**p38**	**pLCK**	**Ikba**	**pCREB**	**pERK1/2**	**NFkB**	**pS6**
Basophils	0	0	0	0	0	0	0	1	1	1	1	1	1	1	1
CD4$^+$ T	0	0	0	0	0	0	0	1	1	1	1	1	1	1	1
CD4$^+$ T$_{Activated}$	0	0	0	0	0	0	0	1	1	1	1	1	1	1	1
CD4$^+$ T$_{Central\ mem}$	0	0	0	0	0	0	0	1	1	1	1	1	1	1	1
CD4$^+$ T$_{Effector}$	0	0	0	0	0	0	0	1	1	1	1	1	1	1	1
CD4$^+$ T$_{Effector\ mem}$	0	0	0	0	0	0	0	1	1	1	1	1	1	1	1
CD4$^+$ T$_{Naïve}$	0	0	0	0	0	0	0	1	1	1	1	1	1	1	1
Tregs	0	0	0	0	0	0	0	1	1	1	1	1	1	1	1
CD8$^+$ T	0	0	0	0	0	0	0	1	1	1	1	1	1	1	1
CD8$^+$ T$_{Activated}$	0	0	0	0	0	0	0	1	1	1	1	1	1	1	1
CD8$^+$ T$_{Central\ mem}$	0	0	0	0	0	0	0	1	1	1	1	1	1	1	1
CD8$^+$ T$_{Effector}$	0	0	0	0	0	0	0	1	1	1	1	1	1	1	1
CD8$^+$ T$_{Effector\ mem}$	0	0	0	0	0	0	0	1	1	1	1	1	1	1	1
CD8$^+$ T$_{Naïve}$	0	0	0	0	0	0	0	1	1	1	1	1	1	1	1
B	0	0	0	0	0	0	0	1	1	1	1	1	1	1	1

IgA^{+} B	0	0	0	0	0	0	1	1	1	1	1	1	1	1	1
IgD^{+} B_{mem}	0	0	0	0	0	0	1	1	1	1	1	1	1	1	1
$IgD^{-}CD27^{-}$ B	0	0	0	0	0	0	1	1	1	1	1	1	1	1	1
$B_{Naïve}$	0	0	0	0	0	0	1	1	1	1	1	1	1	1	1
Plasmablast	0	0	0	0	0	0	1	1	1	1	1	1	1	1	1
$B_{Switched\ mem}$	0	0	0	0	0	0	1	1	1	1	1	1	1	1	1
$B_{Transitional}$	0	0	0	0	0	0	1	1	1	1	1	1	1	1	1
DCs	0	0	0	0	0	0	1	1	1	1	1	1	1	1	1
mDCs	0	0	0	0	0	0	1	1	1	1	1	1	1	1	1
pDCs	0	0	0	0	0	0	1	1	1	1	1	1	1	1	1
NK	0	0	0	0	0	0	1	1	1	1	1	1	1	1	1
$CD16^{high}$ NK	0	0	0	0	0	0	1	1	1	1	1	1	1	1	1
$CD56^{bright}$ NK	0	0	0	0	0	0	1	1	1	1	1	1	1	1	1
$CD56^{dim}CD16^{dim}$ NK	0	0	0	0	0	0	1	1	1	1	1	1	1	1	1
NKT	0	0	0	0	0	0	1	1	1	1	1	1	1	1	1
Mono	0	0	0	0	0	0	1	1	1	1	1	1	1	1	1
$CD16^{low}$ Mono	0	0	0	0	0	0	1	1	1	1	1	1	1	1	1
$CD16^{high}$ Mono	0	0	0	0	0	0	1	1	1	1	1	1	1	1	1

REFERENCES AND NOTES

1. O. Butovsky, M. Koronyo-Hamaoui, G. Kunis, E. Ophir, G. Landa, H. Cohen, M. Schwartz, Glatiramer acetate fights against Alzheimer's disease by inducing dendritic-like microglia expressing insulin-like growth factor 1. *Proc. Natl. Acad. Sci. U.S.A.* **103**, 11784–11789 (2006).

2. M. Fiala, Q. N. Liu, J. Sayre, V. Pop, V. Brahmandam, M. C. Graves, H. V. Vinters, Cyclooxygenase-2-positive macrophages infiltrate the Alzheimer's disease brain and damage the blood-brain barrier. *Eur. J. Clin. Invest.* **32**, 360–371 (2002).

3. T. J. Lewis, C. L. Trempe, *The End of Alzheimer's: The Brain and Beyond* (Academic Press, 2017).

4. R. Perneczky, *Biomarkers for Alzheimer's Disease Drug Development* (Humana Press, 2018).

5. K. Rezai-Zadeh, D. Gate, C. A. Szekely, T. Town, Can peripheral leukocytes be used as Alzheimer's disease biomarkers? *Expert Rev. Neurother.* **9**, 1623–1633 (2009).

6. T. Raj, K. Rothamel, S. Mostafavi, C. Ye, M. N. Lee, J. M. Replogle, T. Feng, M. Lee, N. Asinovski, I. Frohlich, S. Imboywa, A. Von Korff, Y. Okada, N. A. Patsopoulos, S. Davis, C. McCabe, H.-I. Paik, G. P. Srivastava, S. Raychaudhuri, D. A. Hafler, D. Koller, A. Regev, N. Hacohen, D. Mathis, C. Benoist, B. E. Stranger, P. L. De Jager, Polarization of the effects of autoimmune and neurodegenerative risk alleles in leukocytes. *Science* **344**, 519–523 (2014).

7. K. J. Ryan, C. C. White, K. Patel, J. Xu, M. Olah, J. M. Replogle, M. Frangieh, M. Cimpean, P. Winn, A. McHenry, B. J. Kaskow, G. Chan, N. Cuerdon, D. A. Bennett, J. D. Boyd, J. Imitola, W. Elyaman, P. L. De Jager, E. M. Bradshaw, A human microglia-like cellular model for assessing the effects of neurodegenerative disease gene variants. *Sci. Transl. Med.* **9**, eaai7635 (2017).

8. E. Delvaux, D. Mastroeni, J. Nolz, N. Chow, M. Sabbagh, R. J. Caselli, E. M. Reiman, F. J. Marshall, P. D. Coleman, Multivariate analyses of peripheral blood leukocyte transcripts distinguish Alzheimer's, Parkinson's, control, and those at risk for developing Alzheimer's. *Neurobiol. Aging* **58**, 225–237 (2017).

9. G. Schmidbauer, W. W. Hancock, B. Wasowska, A. M. Badger, J. W. Kupiec-Weglinski, Abrogation by rapamycin of accelerated rejection in sensitized rats by inhibition of alloantibody responses and selective suppression of intragraft mononuclear and endothelial cell activation, cytokine production, and cell adhesion. *Transplantation* **57**, 933–941 (1994).

10. R. Davies, P. Vogelsang, R. Jonsson, S. Appel, An optimized multiplex flow cytometry protocol for the analysis of intracellular signaling in peripheral blood mononuclear cells. *J. Immunol. Methods* **436**, 58–63 (2016).

11. S. Ray, M. Britschgi, C. Herbert, Y. Takeda-Uchimura, A. Boxer, K. Blennow, L. F. Friedman, D. R. Galasko, M. Jutel, A. Karydas, J. A. Kaye, J. Leszek, B. L. Miller, L. Minthon, J. F. Quinn, G. D. Rabinovici, W. H. Robinson, M. N. Sabbagh, Y. T. So, D. L. Sparks, M. Tabaton, J. Tinklenberg, J. A. Yesavage, R. Tibshirani, T. Wyss-Coray, Classification and prediction of clinical Alzheimer's diagnosis based on plasma signaling proteins. *Nat. Med.* **13**, 1359–1362 (2007).

12. H. D. Soares, Y. Chen, M. Sabbagh, A. Rohrer, E. Schrijvers, M. Breteler, Identifying early markers of Alzheimer's disease using quantitative multiplex proteomic immunoassay panels. *Ann. N. Y. Acad. Sci.* **1180**, 56–67 (2009).

13. A. Cosma, G. Nolan, B. Gaudilliere, Mass cytometry: The time to settle down. *Cytometry A* **91**, 12–13 (2017).

14. Q. Baca, A. Cosma, G. Nolan, B. Gaudilliere, The road ahead: Implementing mass cytometry in clinical studies, one cell at a time. *Cytometry B Clin. Cytom.* **92**, 10–11 (2017).

15. P. Kvistborg, C. Gouttefangeas, N. Aghaeepour, A. Cazaly, P. K. Chattopadhyay, C. Chan, J. Eckl, G. Finak, S. R. Hadrup, H. T. Maecker, D. Maurer, T. Mosmann, P. Qiu, R. H. Scheuermann, M. J. P. Welters, G. Ferrari, R. R. Brinkman, C. M. Britten, Thinking outside the gate: Single-cell assessments in multiple dimensions. *Immunity* **42**, 591–592 (2015).

16. S. C. Bendall, G. P. Nolan, M. Roederer, P. K. Chattopadhyay, A deep profiler's guide to cytometry. *Trends Immunol.* **33**, 323–332 (2012).

17. N. Aghaeepour, P. Chattopadhyay, M. Chikina, T. Dhaene, S. Van Gassen, M. Kursa, B. N. Lambrecht, M. Malek, G. J. McLachlan, Y. Qian, P. Qiu, Y. Saeys, R. Stanton, D. Tong, C. Vens, S. Walkowiak, K. Wang, G. Finak, R. Gottardo, T. Mosmann, G. P. Nolan, R. H. Scheuermann, R. R. Brinkman, A benchmark for evaluation of algorithms for identification of cellular correlates of clinical outcomes. *Cytometry A* **89**, 16–21 (2016).

18. N. Stanley, I. Stelzer, R. Fallahzadeh, E. Ganio, A. Tsai, M. Becker, T. Phongpreecha, H. Nassar, S. Ghaemi, A. Culos, X. Han, K. Rumer, L. Peterson, A. Chang, I. Maric, D. Gaudilliere, E. Tsai, K. Ando, M. Leipold, G. Bermoser, D. Cross, A. Pollard, H. Maecker, G. Shaw, D. Stevenson, M. Angst, B. Gaudilliere, N. Aghaeepour, VoPo leverages cellular heterogeneity for predictive modeling of single-cell data. *Nat. Commun.* **11**, 3738 (2020).

19. V. G. Tusher, R. Tibshirani, G. Chu, Significance analysis of microarrays applied to the ionizing radiation response. *Proc. Natl. Acad. Sci. U.S.A.* **98**, 5116–5121 (2001).

20. A. E. Culos, A. S. Tsai, N. Stanley, M. Becker, M. S. Ghaemi, D. R. Mcilwain, R. Fallahzadeh, A. Tanada, H. Nassar, E. Ganio, L. Peterson, X. Han, I. Stelzer, K. Ando, D. Gaudilliere, T. Phongpreecha, I. Marić, A. L. Chang, G. M. Shaw, D. K. Stevenson, S. Bendall, K. L. Davis, W. Fantl, G. P. Nolan, T. Hastie, R. Tibshirani, M. S. Angst, B. Gaudilliere, N. Aghaeepour, Integration of mechanistic immunological knowledge into a machine learning pipeline improves predictions. *Nat. Mach. Intell.* **2**, 619–628 (2020).

21. R. Sims, S. J. van der Lee, A. C. Naj, C. Bellenguez, N. Badarinarayan, J. Jakobsdottir, B. W. Kunkle, A. Boland, R. Raybould, J. C. Bis, E. R. Martin, B. Grenier-Boley, S. Heilmann-Heimbach, V. Chouraki, A. B. Kuzma, K. Sleegers, M. Vronskaya, A. Ruiz, R. R. Graham, R. Olaso, P. Hoffmann, M. L. Grove, B. N. Vardarajan, M. Hiltunen, M. M. Nöthen, C. C. White, K. L. Hamilton-Nelson, J. Epelbaum, W. Maier, S.-H. Choi, G. W. Beecham, C. Dulary, S. Herms, A. V. Smith, C. C. Funk, C. Derbois, A. J. Forstner, S. Ahmad, H. Li, D. Bacq, D. Harold, C. L. Satizabal, O. Valladares, A. Squassina, R. Thomas, J. A. Brody, L. Qu, P. Sánchez-Juan, T. Morgan, F. J. Wolters, Y. Zhao, F. S. Garcia, N. Denning, M. Fornage, J. Malamon, M. C. D. Naranjo, E. Majounie, T. H. Mosley, B. Dombroski, D. Wallon, M. K. Lupton, J. Dupuis, P. Whitehead, L. Fratiglioni, C. Medway, X. Jian, S. Mukherjee, L. Keller, K. Brown, H. Lin, L. B. Cantwell, F.

Panza, B. McGuinness, S. Moreno-Grau, J. D. Burgess, V. Solfrizzi, P. Proitsi, H. H. Adams, M. Allen, D. Seripa, P. Pastor, L. A. Cupples, N. D. Price, D. Hannequin, A. Frank-García, D. Levy, P. Chakrabarty, P. Caffarra, I. Giegling, A. S. Beiser, V. Giedraitis, H. Hampel, M. E. Garcia, X. Wang, L. Lannfelt, P. Mecocci, G. Eiriksdottir, P. K. Crane, F. Pasquier, V. Boccardi, I. Henández, R. C. Barber, M. Scherer, L. Tarraga, P. M. Adams, M. Leber, Y. Chen, M. S. Albert, S. Riedel-Heller, V. Emilsson, D. Beekly, A. Braae, R. Schmidt, D. Blacker, C. Masullo, H. Schmidt, R. S. Doody, G. Spalletta, W. T. Longstreth Jr., T. J. Fairchild, P. Bossù, O. L. Lopez, M. P. Frosch, E. Sacchinelli, B. Ghetti, Q. Yang, R. M. Huebinger, F. Jessen, S. Li, M. I. Kamboh, J. Morris, O. Sotolongo-Grau, M. J. Katz, C. Corcoran, M. Dunstan, A. Braddel, C. Thomas, A. Meggy, R. Marshall, A. Gerrish, J. Chapman, M. Aguilar, S. Taylor, M. Hill, M. D. Fairén, A. Hodges, B. Vellas, H. Soininen, I. Kloszewska, M. Daniilidou, J. Uphill, Y. Patel, J. T. Hughes, J. Lord, J. Turton, A. M. Hartmann, R. Cecchetti, C. Fenoglio, M. Serpente, M. Arcaro, C. Caltagirone, M. D. Orfei, A. Ciaramella, S. Pichler, M. Mayhaus, W. Gu, A. Lleó, J. Fortea, R. Blesa, I. S. Barber, K. Brookes, C. Cupidi, R. G. Maletta, D. Carrell, S. Sorbi, S. Moebus, M. Urbano, A. Pilotto, J. Kornhuber, P. Bosco, S. Todd, D. Craig, J. Johnston, M. Gill, B. Lawlor, A. Lynch, N. C. Fox, J. Hardy, ARUK Consortium, R. L. Albin, L. G. Apostolova, S. E. Arnold, S. Asthana, C. S. Atwood, C. T. Baldwin, L. L. Barnes, S. Barral, T. G. Beach, J. T. Becker, E. H. Bigio, T. D. Bird, B. F. Boeve, J. D. Bowen, A. Boxer, J. R. Burke, J. M. Burns, J. D. Buxbaum, N. J. Cairns, C. Cao, C. S. Carlson, C. M. Carlsson, R. M. Carney, M. M. Carrasquillo, S. L. Carroll, C. C. Diaz, H. C. Chui, D. G. Clark, D. H. Cribbs, E. A. Crocco, C. DeCarli, M. Dick, R. Duara, D. A. Evans, K. M. Faber, K. B. Fallon, D. W. Fardo, M. R. Farlow, S. Ferris, T. M. Foroud, D. R. Galasko, M. Gearing, D. H. Geschwind, J. R. Gilbert, N. R. Graff-Radford, R. C. Green, J. H. Growdon, R. L. Hamilton, L. E. Harrell, L. S. Honig, M. J. Huentelman, C. M. Hulette, B. T. Hyman, G. P. Jarvik, E. Abner, L.-W. Jin, G. Jun, A. Karydas, J. A. Kaye, R. Kim, N. W. Kowall, J. H. Kramer, F. M. LaFerla, J. J. Lah, J. B. Leverenz, A. I. Levey, G. Li, A. P. Lieberman, K. L. Lunetta, C. G. Lyketsos, D. C. Marson, F. Martiniuk, D. C. Mash, E. Masliah, W. C. McCormick, S. M. McCurry, A. N. McDavid, A. C. McKee, M. Mesulam, B. L. Miller, C. A. Miller, J. W. Miller, J. C. Morris, J. R. Murrell, A. J. Myers, S. O'Bryant, J. M. Olichney, V. S. Pankratz, J. E. Parisi, H. L. Paulson, W. Perry, E. Peskind, A. Pierce, W. W. Poon, H. Potter, J. F. Quinn, A. Raj, M. Raskind, B. Reisberg, C. Reitz, J. M. Ringman, E. D. Roberson, E. Rogaeva, H. J. Rosen, R. N. Rosenberg, M. A. Sager, A. J. Saykin, J. A. Schneider, L. S. Schneider, W. W. Seeley, A. G. Smith, J. A. Sonnen, S. Spina, R. A. Stern, R.

H. Swerdlow, R. E. Tanzi, T. A. Thornton-Wells, J. Q. Trojanowski, J. C. Troncoso, V. M. Van Deerlin, L. J. Van Eldik, H. V. Vinters, J. P. Vonsattel, S. Weintraub, K. A. Welsh-Bohmer, K. C. Wilhelmsen, J. Williamson, T. S. Wingo, R. L. Woltjer, C. B. Wright, C.-E. Yu, L. Yu, F. Garzia, F. Golamaully, G. Septier, S. Engelborghs, R. Vandenberghe, P. P. De Deyn, C. M. Fernadez, Y. A. Benito, H. Thonberg, C. Forsell, L. Lilius, A. Kinhult-Stählbom, L. Kilander, R. Brundin, L. Concari, S. Helisalmi, A. M. Koivisto, A. Haapasalo, V. Dermecourt, N. Fievet, O. Hanon, C. Dufouil, A. Brice, K. Ritchie, B. Dubois, J. J. Himali, C. D. Keene, J. Tschanz, A. L. Fitzpatrick, W. A. Kukull, M. Norton, T. Aspelund, E. B. Larson, R. Munger, J. I. Rotter, R. B. Lipton, M. J. Bullido, A. Hofman, T. J. Montine, E. Coto, E. Boerwinkle, R. C. Petersen, V. Alvarez, F. Rivadeneira, E. M. Reiman, M. Gallo, C. J. O'Donnell, J. S. Reisch, A. C. Bruni, D. R. Royall, M. Dichgans, M. Sano, D. Galimberti, P. St George-Hyslop, E. Scarpini, D. W. Tsuang, M. Mancuso, U. Bonuccelli, A. R. Winslow, A. Daniele, C.-K. Wu; GERAD/PERADES, CHARGE, ADGC, EADI, O. Peters, B. Nacmias, M. Riemenschneider, R. Heun, C. Brayne, D. C. Rubinsztein, J. Bras, R. Guerreiro, A. Al-Chalabi, C. E. Shaw, J. Collinge, D. Mann, M. Tsolaki, J. Clarimón, R. Sussams, S. Lovestone, M. C. O'Donovan, M. J. Owen, T. W. Behrens, S. Mead, A. M. Goate, A. G. Uitterlinden, C. Holmes, C. Cruchaga, M. Ingelsson, D. A. Bennett, J. Powell, T. E. Golde, C. Graff, P. L. De Jager, K. Morgan, N. Ertekin-Taner, O. Combarros, B. M. Psaty, P. Passmore, S. G. Younkin, C. Berr, V. Gudnason, D. Rujescu, D. W. Dickson, J.-F. Dartigues, A. L. DeStefano, S. Ortega-Cubero, H. Hakonarson, D. Campion, M. Boada, J. K. Kauwe, L. A. Farrer, C. Van Broeckhoven, M. A. Ikram, L. Jones, J. L. Haines, C. Tzourio, L. J. Launer, V. Escott-Price, R. Mayeux, J.-F. Deleuze, N. Amin, P. A. Holmans, M. A. Pericak-Vance, P. Amouyel, C. M. van Duijn, A. Ramirez, L.-S. Wang, J.-C. Lambert, S. Seshadri, J. Williams, G. D. Schellenberg, Rare coding variants in *PLCG2*, ABI3, and TREM2 implicate microglial-mediated innate immunity in Alzheimer's disease. *Nat. Genet.* **49**, 1373–1384 (2017).

22. C. Le Saout, M. A. Luckey, A. V. Villarino, M. Smith, R. B. Hasley, T. G. Myers, H. Imamichi, J.-H. Park, J. J. O'Shea, H. C. Lane, M. Catalfamo, IL-7-dependent STAT1 activation limits homeostatic $CD4^+$ T cell expansion. *JCI Insight* **2**, e96228 (2017).

23. G. K. Fragiadakis, Z. B. Bjornson-Hooper, D. Madhireddy, K. Sachs, M. H. Spitzer, S. C. Bendall, G. P. Nolan, Variation of immune cell responses in humans reveals sex-specific coordinated signaling across cell types. *bioRxiv*, 567784 (2019).

24. J. R. Lynch, W. Tang, H. Wang, M. P. Vitek, E. R. Bennett, P. M. Sullivan, D. S. Warner, D. T. Laskowitz, APOE genotype and an ApoE-mimetic peptide modify the systemic and central nervous system inflammatory response. *J. Biol. Chem.* **278**, 48529–48533 (2003).

25. M. P. Vitek, C. M. Brown, C. A. Colton, APOE genotype-specific differences in the innate immune response. *Neurobiol. Aging* **30**, 1350–1360 (2009).

26. R. W. Mahley, S. C. Rall Jr., Apolipoprotein E: Far more than a lipid transport protein. *Annu. Rev. Genomics Hum. Genet.* **1**, 507–537 (2000).

27. P. Olgiati, A. Politis, P. Malitas, D. Albani, S. Dusi, L. Polito, S. De Mauro, A. Zisaki, C. Piperi, E. Stamouli, A. Mailis, S. Batelli, G. Forloni, D. De Ronchi, A. Kalofoutis, I. Liappas, A. Serretti, APOE epsilon-4 allele and cytokine production in Alzheimer's disease. *Int. J. Geriatr. Psychiatry* **25**, 338–344 (2010).

28. D. Gate, N. Saligrama, O. Leventhal, A. C. Yang, M. S. Unger, J. Middeldorp, K. Chen, B. Lehallier, D. Channappa, M. B. De Los Santos, A. McBride, J. Pluvinage, F. Elahi, G. K.-Y. Tam, Y. Kim, M. Greicius, A. D. Wagner, L. Aigner, D. R. Galasko, M. M. Davis, T. Wyss-Coray, Clonally expanded CD8 T cells patrol the cerebrospinal fluid in Alzheimer's disease. *Nature* **577,** 399–404 (2020).

29. C. R. Stewart, L. M. Stuart, K. Wilkinson, J. M. van Gils, J. Deng, A. Halle, K. J. Rayner, L. Boyer, R. Zhong, W. A. Frazier, A. Lacy-Hulbert, J. El Khoury, D. T. Golenbock, K. J. Moore, CD36 ligands promote sterile inflammation through assembly of a Toll-like receptor 4 and 6 heterodimer. *Nat. Immunol.* **11**, 155–161 (2010).

30. K. Fujita, K. Motoki, K. Tagawa, X. Chen, H. Hama, K. Nakajima, H. Homma, T. Tamura, H. Watanabe, M. Katsuno, C. Matsumi, M. Kajikawa, T. Saito, T. Saido, G. Sobue, A. Miyawaki, H. Okazawa, HMGB1, a pathogenic molecule that induces neurite degeneration via TLR4-MARCKS, is a potential therapeutic target for Alzheimer's disease. *Sci. Rep.* **6**, 31895 (2016).

31. Y. Kitamura, S. Shimohama, T. Ota, Y. Matsuoka, Y. Nomura, T. Taniguchi, Alteration of transcription factors NF-κB and STAT1 in Alzheimer's disease brains. *Neurosci. Lett.* **237**, 17–20 (1997).

32. W. J. Lee, S. A. Ham, G. H. Lee, M. Choi, H. Yoo, K. S. Paek, D. Lim, K. Hong, J. S. Hwang, H. G. Seo, Activation of peroxisome proliferator-activated receptor delta suppresses BACE 1 expression by up-regulating SOCS 1 in a JAK2/ STAT1-dependent manner. *J. Neurochem.* **151**, 370–385 (2019).

33. G. Di Liberto, S. Pantelyushin, M. Kreutzfeldt, N. Page, S. Musardo, R. Coras, K. Steinbach, I. Vincenti, B. Klimek, T. Lingner, G. Salinas, N. Lin-Marq, O. Staszewski, M. J. Costa Jordão, I. Wagner, K. Egervari, M. Mack, C. Bellone, I. Blümcke, M. Prinz, D. D. Pinschewer, D. Merkler, Neurons under T cell attack coordinate phagocyte-mediated synaptic stripping. *Cell* **175**, 458–471.e19 (2018).

34. A. J. Nevado-Holgado, E. Ribe, L. Thei, L. Furlong, M.-A. Mayer, J. Quan, J. C. Richardson, J. Cavanagh, N. Consortium, S. Lovestone, Genetic and real-world clinical data, combined with empirical validation, nominate JAK-STAT signaling as a target for Alzheimer's disease therapeutic development. *Cell* **8**, 425 (2019).

35. O. J. Conway, M. M. Carrasquillo, X. Wang, J. M. Bredenberg, J. S. Reddy, S. L. Strickland, C. S. Younkin, J. D. Burgess, M. Allen, S. J. Lincoln, T. Nguyen, K. G. Malphrus, A. I. Soto, R. L. Walton, B. F. Boeve, R. C. Petersen, J. A. Lucas, T. J. Ferman, W. P. Cheshire, J. A. van Gerpen, R. J. Uitti, Z. K. Wszolek, O. A. Ross, D. W. Dickson, N. R. Graff-Radford, N. Ertekin-Taner, *ABI3* and *PLCG2* missense variants as risk factors for neurodegenerative diseases in Caucasians and African Americans. *Mol. Neurodegener.* **13**, 53 (2018).

36. S. J. van der Lee, O. J. Conway, I. Jansen, M. M. Carrasquillo, L. Kleineidam, E. van den Akker, I. Hernández, K. R. van Eijk, N. Stringa, J. A. Chen, A. Zettergren, T. F. M. Andlauer, M. Diez-Fairen, J. Simon-Sanchez, A. Lleó, H. Zetterberg, M. Nygaard, C. Blauwendraat, J. E. Savage, J. Mengel-From, S. Moreno-Grau, M. Wagner, J. Fortea, M. J. Keogh, K. Blennow, I. Skoog, M. A. Friese, O. Pletnikova, M. Zulaica, C. Lage, I. de Rojas, S. Riedel-Heller, I. Illán-Gala, W. Wei, B. Jeune, A. Orellana, F. Then Bergh, X. Wang, M. Hulsman, N. Beker, N. Tesi, C. M. Morris, B. Indakoetxea,

L. E. Collij, M. Scherer, E. Morenas-Rodríguez, J. W. Ironside, B. N. M. van Berckel, D. Alcolea, H. Wiendl, S. L. Strickland, P. Pastor, E. Rodríguez Rodríguez; DESGESCO (Dementia Genetics Spanish Consortium), EADB (Alzheimer Disease European DNA biobank), EADB (Alzheimer Disease European DNA biobank), IFGC (International FTD-Genomics Consortium), IPDGC (The International Parkinson Disease Genomics Consortium), IPDGC (The International Parkinson Disease Genomics Consortium), RiMod-FTD (Risk and Modifying factors in Fronto-Temporal Dementia), Netherlands Brain Bank (NBB), B. F. Boeve, R. C. Petersen, T. J. Ferman, J. A. van Gerpen, M. J. T. Reinders, R. J. Uitti, L. Tárraga, W. Maier, O. Dols-Icardo, A. Kawalia, M. C. Dalmasso, M. Boada, U. K. Zettl, N. M. van Schoor, M. Beekman, M. Allen, E. Masliah, A. L. de Munain, A. Pantelyat, Z. K. Wszolek, O. A. Ross, D. W. Dickson, N. R. Graff-Radford, D. Knopman, R. Rademakers, A. W. Lemstra, Y. A. L. Pijnenburg, P. Scheltens, T. Gasser, P. F. Chinnery, B. Hemmer, M. A. Huisman, J. Troncoso, F. Moreno, E. A. Nohr, T. I. A. Sørensen, P. Heutink, P. Sánchez-Juan, D. Posthuma; GIFT (Genetic Investigation in Frontotemporal Dementia and Alzheimer's Disease) Study Group, J. Clarimón, K. Christensen, N. Ertekin-Taner, S. W. Scholz, A. Ramirez, A. Ruiz, E. Slagboom, W. M. van der Flier, H. Holstege, A nonsynonymous mutation in *PLCG2* reduces the risk of Alzheimer's disease, dementia with Lewy bodies and frontotemporal dementia, and increases the likelihood of longevity. *Acta Neuropathol.* **138**, 237–250 (2019).

37. M. C. Dalmasso, L. I. Brusco, N. Olivar, C. Muchnik, C. Hanses, E. Milz, J. Becker, S. Heilmann-Heimbach, P. Hoffmann, F. A. Prestia, P. Galeano, M. S. S. Avalos, L. E. Martinez, M. E. Carulla, P. J. Azurmendi, C. Liberczuk, C. Fezza, M. Sampaño, M. Fierens, G. Jemar, P. Solis, N. Medel, J. Lisso, Z. Sevillano, P. Bosco, P. Bossù, G. Spalletta, D. Galimberti, M. Mancuso, B. Nacmias, S. Sorbi, P. Mecocci, A. Pilotto, P. Caffarra, F. Panza, M. Bullido, J. Clarimon, P. Sánchez-Juan, E. Coto, F. Sanchez-Garcia, C. Graff, M. Ingelsson, C. Bellenguez, E. M. Castaño, C. Kairiyama, D. G. Politis, S. Kochen, H. Scaro, W. Maier, F. Jessen, C. A. Mangone, J.-C. Lambert, L. Morelli, A. Ramirez, Transethnic meta-analysis of rare coding variants in *PLCG2*, *ABI3*, and *TREM2* supports their general contribution to Alzheimer's disease. *Transl. Psychiatry* **9**, 55 (2019).

38. L. Magno, C. B. Lessard, M. Martins, P. Cruz, M. Katan, J. Bilsland, P. Chakrabaty, T. E. Golde, P. Whiting, Alzheimer's disease phospholipase C-gamma-2 (PLCG2) protective variant is a functional hypermorph. *Alzheimers Res. Ther.* **11**, 16 (2019).

39. J. D. Milner, PLAID: A syndrome of complex patterns of disease and unique phenotypes. *J. Clin. Immunol.* **35**, 527–530 (2015).

40. A. Nott, I. R. Holtman, N. G. Coufal, J. C. M. Schlachetzki, M. Yu, R. Hu, C. Z. Han, M. Pena, J. Xiao, Y. Wu, Z. Keulen, M. P. Pasillas, C. O'Connor, C. K. Nickl, S. T. Schafer, Z. Shen, R. A. Rissman, J. B. Brewer, D. Gosselin, D. D. Gonda, M. L. Levy, M. G. Rosenfeld, G. McVicker, F. H. Gage, B. Ren, C. K. Glass, Brain cell type–specific enhancer-promoter interactome maps and disease risk association. *Science* **366**, 1134–1139 (2019).

41. T. E. Golde, Harnessing immunoproteostasis to treat neurodegenerative disorders. *Neuron* **101**, 1003–1015 (2019).

42. I. Litvan, K. P. Bhatia, D. J. Burn, C. G. Goetz, A. E. Lang, I. McKeith, N. Quinn, K. D. Sethi, C. Shults, G. K. Wenning; Movement Disorders Society Scientific Issues Committee, Movement Disorders Society Scientific Issues Committee report: SIC Task Force appraisal of clinical diagnostic criteria for parkinsonian disorders. *Mov. Disord.* **18**, 467–486 (2003).

43. B. A. Cholerton, C. P. Zabetian, J. F. Quinn, K. A. Chung, A. Peterson, A. J. Espay, F. J. Revilla, J. Devoto, G. Watson, S. C. Hu, K. L. Edwards, T. J. Montine, J. B. Leverenz, Pacific Northwest Udall Center of excellence clinical consortium: Study design and baseline cohort characteristics. *J. Parkinsons Dis.* **3**, 205–214 (2013).

44. G. M. McKhann, D. S. Knopman, H. Chertkow, B. T. Hyman, C. R. Jack, C. H. Kawas, W. E. Klunk, W. J. Koroshetz, J. J. Manly, R. Mayeux, R. C. Mohs, J. C. Morris, M. N. Rossor, P. Scheltens, M. C. Carrillo, B. Thies, S. Weintraub, C. H. Phelps, The diagnosis of dementia due to Alzheimer's disease: Recommendations from the National Institute on Aging-Alzheimer's Association workgroups on diagnostic guidelines for Alzheimer's disease. *Alzheimers Dement.* **7**, 263–269 (2011).

45. H. W. Grievink, T. Luisman, C. Kluft, M. Moerland, K. E. Malone, Comparison of three isolation techniques for human peripheral blood mononuclear cells: Cell recovery and viability, population composition, and cell functionality. *Biopreserv. Biobank.* **14**, 410–415 (2016).

46. R. Fernandez, H. Maecker, Cytokine-stimulated phosphoflow of PBMC using CyTOF mass cytometry. *Bio Protoc.* **5**, e1496 (2015).

47. E. R. Zunder, R. Finck, G. K. Behbehani, E.-A. D. Amir, S. Krishnaswamy, V. D. Gonzalez, C. G. Lorang, Z. Bjornson, M. H. Spitzer, B. Bodenmiller, W. J. Fantl, D. Pe'er, G. P. Nolan, Palladium-based mass tag cell barcoding with a doublet-filtering scheme and single-cell deconvolution algorithm. *Nat. Protoc.* **10**, 316–333 (2015).

48. J. Choi, R. Fernandez, H. T. Maecker, M. J. Butte, Systems approach to uncover signaling networks in primary immunodeficiency diseases. *J. Allergy Clin. Immunol.* **140**, 881–884.e8 (2017).

49. S. C. Bendall, E. F. Simonds, P. Qiu, E.-A. D. Amir, P. O. Krutzik, R. Finck, R. V. Bruggner, R. Melamed, A. Trejo, O. I. Ornatsky, R. S. Balderas, S. K. Plevritis, K. Sachs, D. Pe'er, S. D. Tanner, G. P. Nolan, Single-cell mass cytometry of differential immune and drug responses across a human hematopoietic continuum. *Science* **332**, 687–696 (2011).

50. R. Finck, E. F. Simonds, A. Jager, S. Krishnaswamy, K. Sachs, W. Fantl, D. Pe'er, G. P. Nolan, S. C. Bendall, Normalization of mass cytometry data with bead standards. *Cytometry A* **83**, 483–494 (2013).

51. W. E. O'Gorman, H. Huang, Y.-L. Wei, K. L. Davis, M. D. Leipold, S. C. Bendall, B. A. Kidd, C. L. Dekker, H. T. Maecker, Y.-H. Chien, M. M. Davis, The split virus influenza vaccine rapidly activates immune cells through Fcγ receptors. *Vaccine* **32**, 5989–5997 (2014).

52. C. L. Galligan, J. C. Siebert, K. A. Siminovitch, E. C. Keystone, V. Bykerk, O. D. Perez, E. N. Fish, Multiparameter phospho-flow analysis of lymphocytes in early rheumatoid arthritis: Implications for diagnosis and monitoring drug therapy. *PLOS ONE* **4**, e6703 (2009).

53. W. Xu, F. Fang, J. Ding, C. Wu, Dysregulation of Rab5-mediated endocytic pathways in Alzheimer's disease. *Traffic* **19**, 253–262 (2018).

54. R. Xavier, N. Turck, A. Hainard, N. Tiberti, F. Lisacek, J. C. Sanchez, M. Müller, pROC: An open-source package for R and S+ to analyze and compare ROC curves. *BMC Bioinformatics* **12**, 77 (2011).

55. C. James, J. Bithell, Bootstrap confidence intervals: When, which, what? A practical guide for medical statisticians. *Stat. Med.* **19**, 1141–1164 (2000).

56. N. A. Obuchowski, M. L. Lieber, F. H. Wians Jr., ROC curves in *Clinical Chemistry*: Uses, misuses, and possible solutions. *Clin. Chem.* **50**, 1118–1125 (2004).

57. M. D. Leipold, E. W. Newell, H. T. Maecker, *Multiparameter Phenotyping of Human PBMCs using Mass Cytometry in Immunosenescence* (Humana Press, 2015), pp. 81–95.

58. W. E. Johnson, C. Li, A. Rabinovic, Adjusting batch effects in microarray expression data using empirical Bayes methods. *Biostatistics* **8**, 118–127 (2007).

59. A. Scherer, *Batch Effects and Noise in Microarray Experiments: Sources and Solutions* (John Wiley & Sons, 2009).

60. D. Di Mitri, R. I. Azevedo, S. M. Henson, V. Libri, N. E. Riddell, R. Macaulay, D. Kipling, M. V. D. Soares, L. Battistini, A. N. Akbar, Reversible senescence in human $CD4^{+}$ $CD45RA^{+}$ $CD27^{-}$ memory T cells. *J. Immunol.* **187**, 2093–2100 (2011).

61. V. M. R. Muggeo, Estimating regression models with unknown break-points. *Stat. Med.* **22**, 3055–3071 (2003).